Phase stability and enhanced hardness in TiN-ScN and TiN-YN alloys: a first-principles investigation

Dr. Sanjay V. Khare

V. Adhikari[a] , N.J. Szymanski[a] , I. Khatri[a] , D. Gall[b] , S.V. Khare[a]

[a]*Department of Physics and Astronomy, University of Toledo, Toledo, Ohio 43606, USA*

[b]*Department of Materials Science and Engineering, Rensselaer Polytechnic Institute, Troy, NY 12180, USA*

Invited Paper: Thin Solid Films 688, 137284 (2019), https://doi.org/10.1016/j.tsf.2019.05.003.

Materials Genome Initiative
WWW.MGI.GOV

Ohio Supercomputer Center

Outlines

- Introduction
- Computational Methods
- Results
- Conclusion

Introduction

Transition Metal Nitrides (TMN) are widely used in hard coatings.

TiN is most widely used TMN for hard coatings: High thermal stability and hardness and low cost of synthesis.

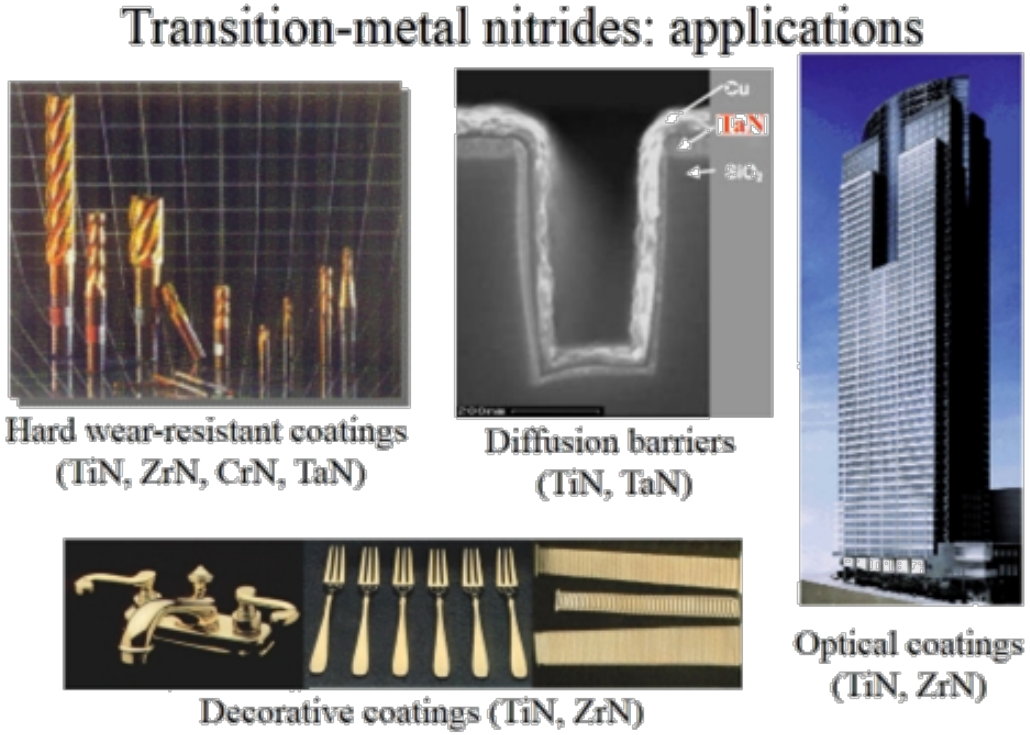

- Wear resistant
- Chemical corrosion/oxidation resistant
- Thermal resistant
- Aesthetically pleasing

Anwers to Driving Questions

- Can we obtain **predictive** physical understanding of stable, hard and tough materials for coatings from first-principles calculations?
  - Thermodynamically (multiple-phase stability)? **Yes**
  - Mechanically (single-phase stability)? **Yes**

- Can we identify trends of properties and possible correlations between them to restrict the parameter search space. **Yes but only when they exist**

- To what extent can we reduce time and effort to experimentally discover and synthesize new materials. **To a good extent for well-defined small unit-cell crystal systems**

Computational Methods

Materials Genome Initiative
WWW.MGI.GOV

Computationally achievable on a large scale

Computationally achievable on case by case basis

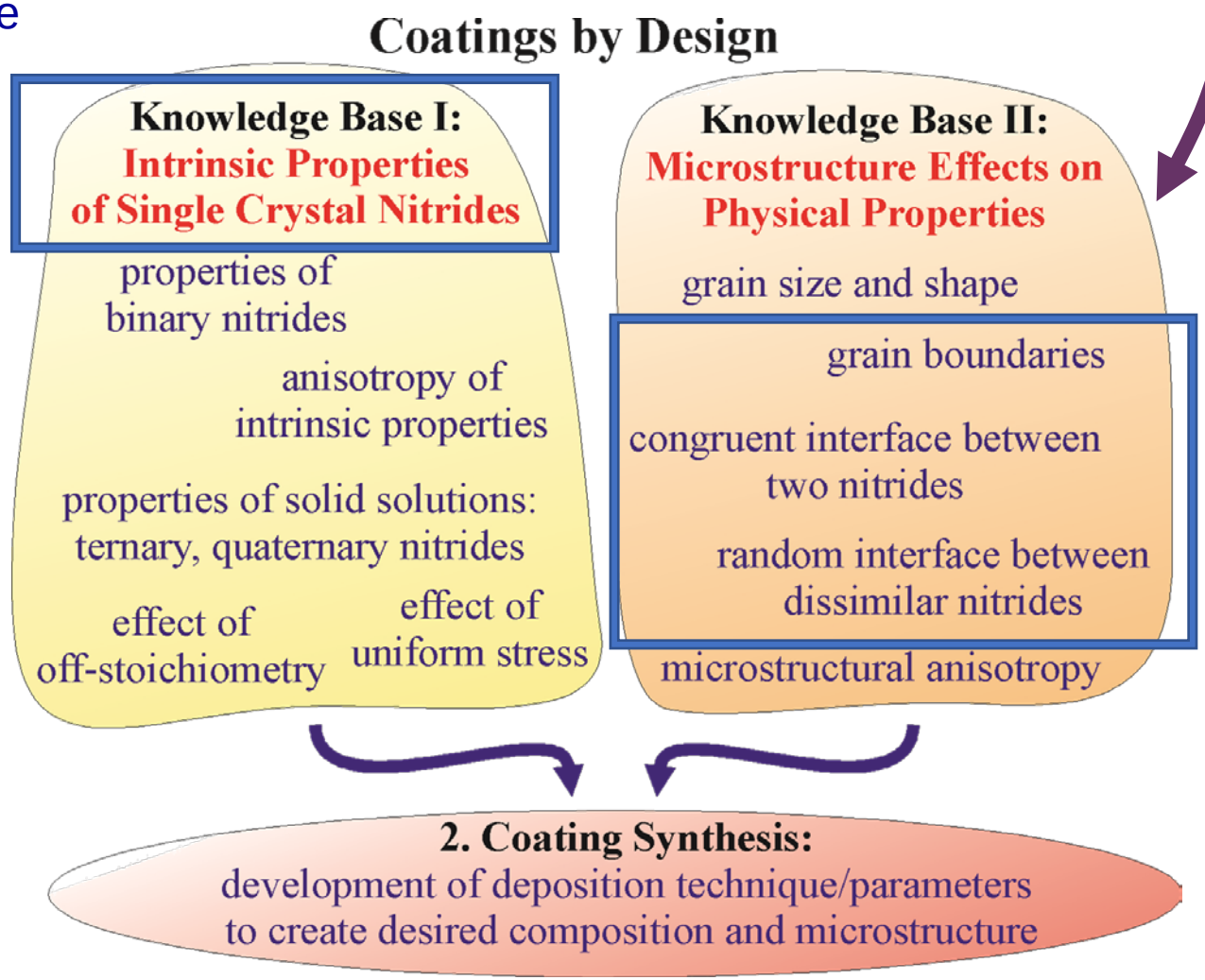

Computational Methods: The general procedure, T = 0 K

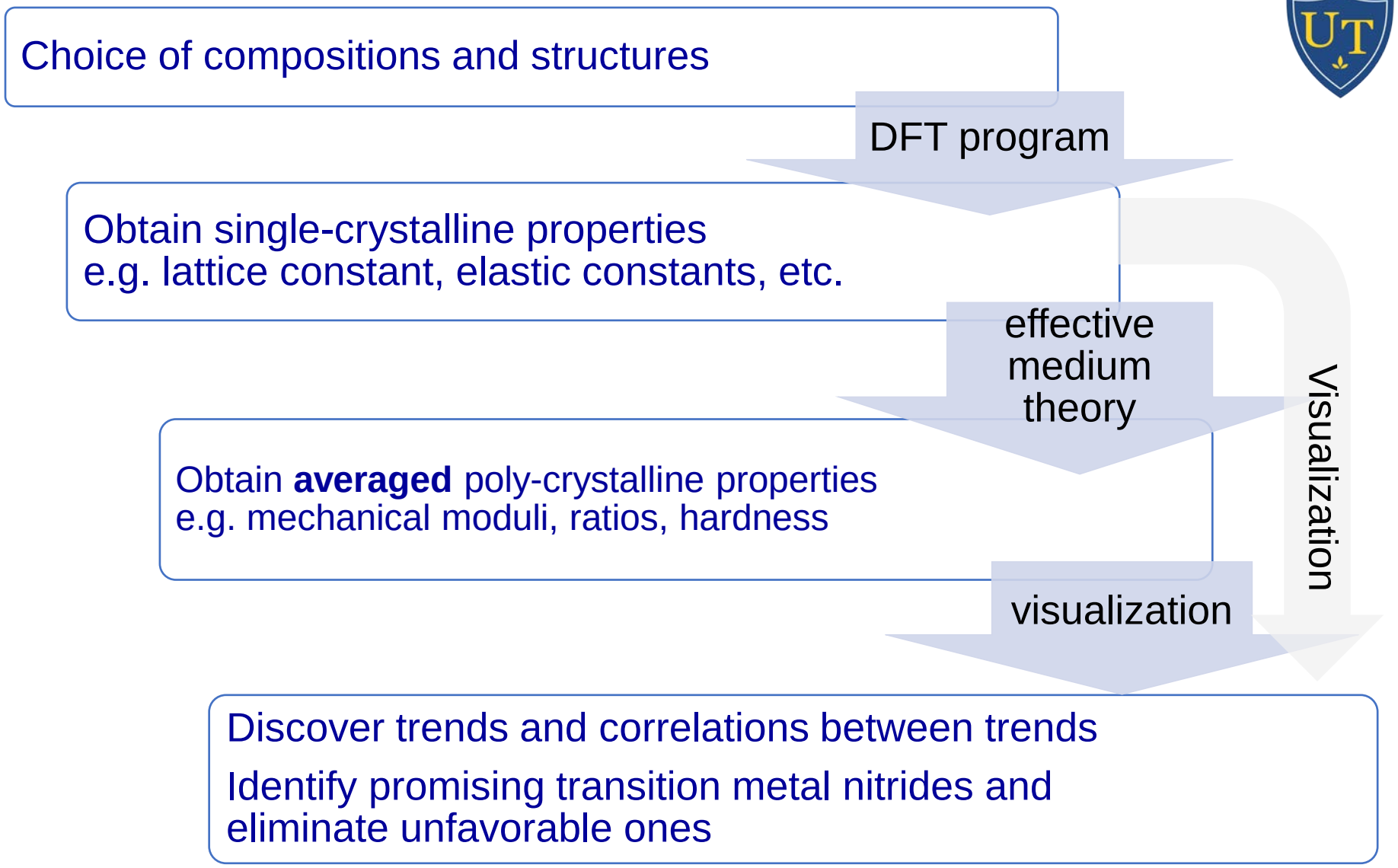

Results: Database generation, T = 0K

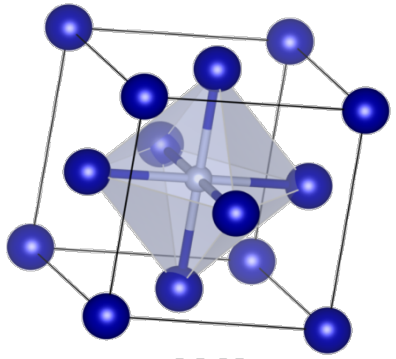

M_4N

4:1

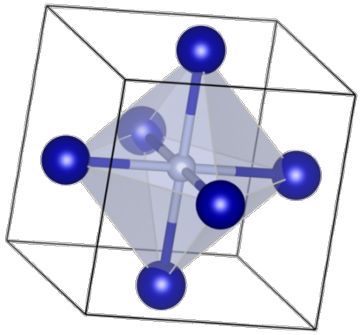

3:1

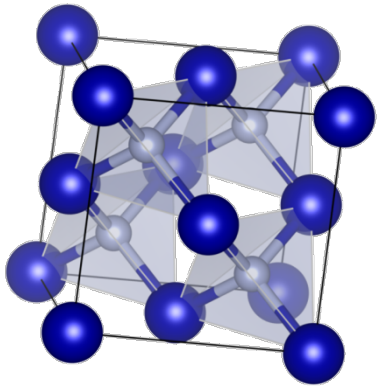

zinc blende

4:4

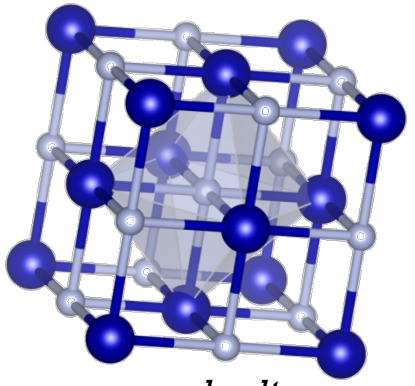

rocksalt

4:4

Several papers came out of this work.

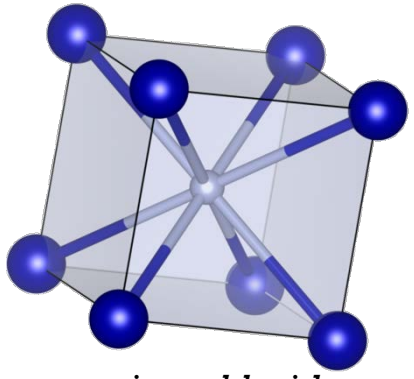

cesium chloride

1:1

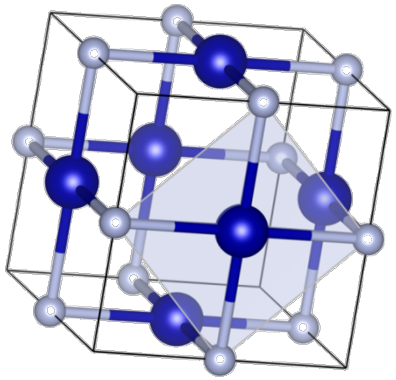

NbO

3:3

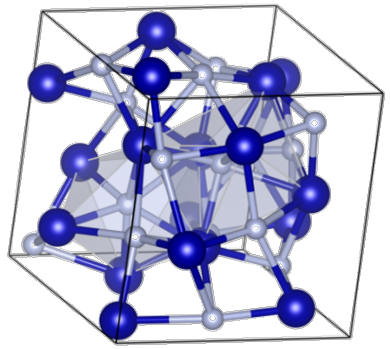

Th_3P_4

3:4

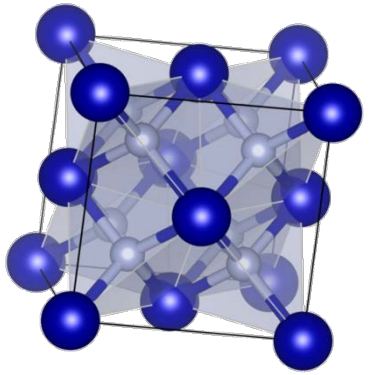

fluorite

4:8

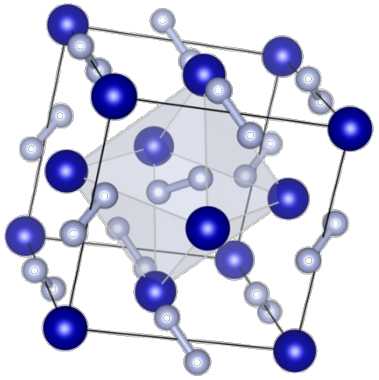

pyrite

4:8

The Grand Scheme of Things: T > 0 K

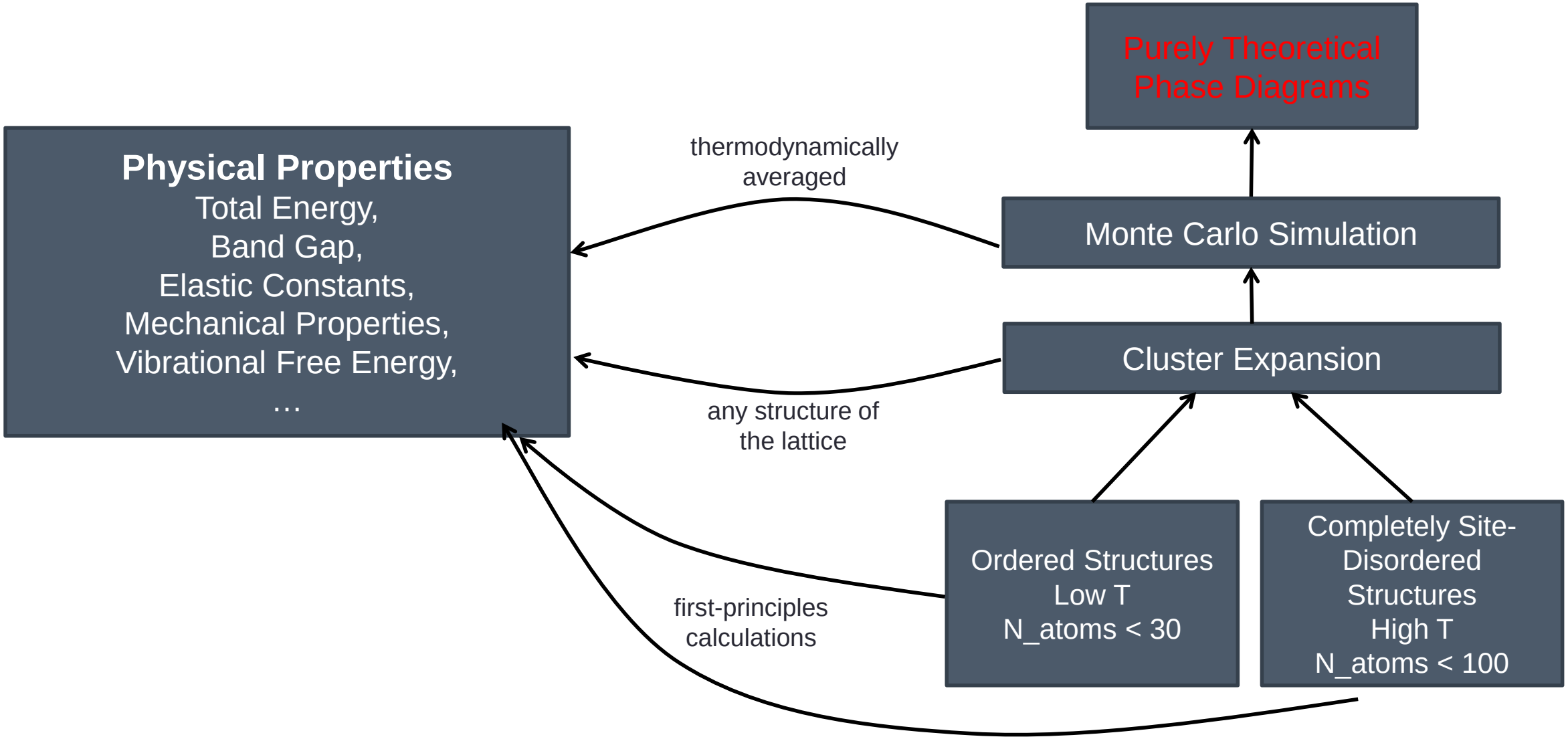

Computational Methods

- Density Functional Theory (DFT)
- Disorder modeling – Special Quasi-random Structure (SQS)
- Temperature-composition phase diagram generation
  - Cluster expansion (CE)
  - Monte Carlo (MC) simulations

Computational Methods

Density Functional Theory (DFT)

- A method to obtain an approximate solution to the Schrodinger Wave Equation for many-body system

- Functional: a function of a function
- In DFT, E = E[ρ(r)], where ρ(r) = ground-state electron density.

- Describing an interacting system of N fermions with it's **density ρ(x,y,z) and not with it's many-body wavefunction φ(x_1,y_1,z_1,……x_N,y_N,z_N)**.

- 3N degree of freedom is reduced to 3.
- The electron density is an observable

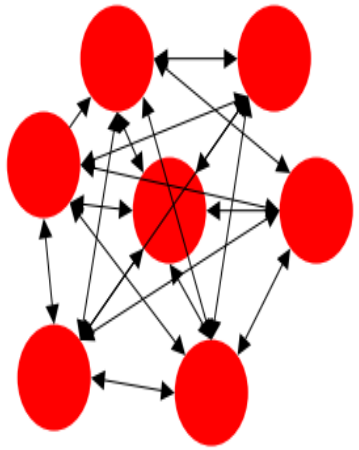

Interacting electrons
+ real potential

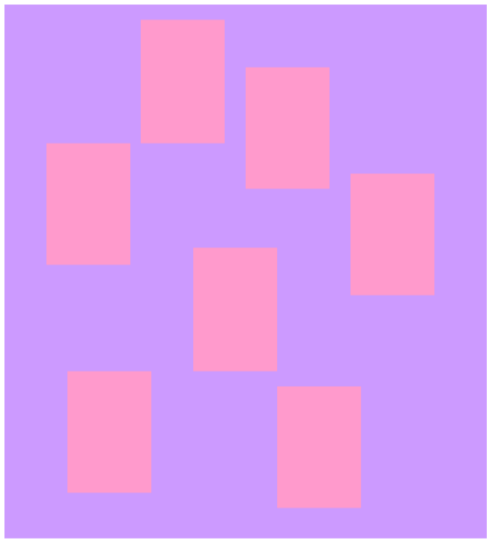

Non-interacting fictitious particles + effective potential

Computational Methods

Disorder modeling – Special Quasi-random Structure (SQS)

- A special quasi-random structure (SQS) is a supercell that matches, or is very close to the correlations of a random state.
- SQS generation with the mcsqs [1] program in The Alloy Theoretic Automated Toolkit (ATAT) [2].
- Inputs are maximum diameter of the pair/triplet/quadruplet clusters to match the supercell size. The more clusters included, the larger the supercell is needed to perfectly match the random state.

[1] A. van de Walle *et al.*, Calphad-Computer Coupling of Phase Diagrams and Thermochemistry **42**, 13 (2013).
[2] A. van de Walle *et al.*, Calphad-Computer Coupling of Phase Diagrams and Thermochemistry **26**, 539 (2002).

Computational Methods: SQS for T very high

- The more clusters included, the larger the supercell is needed to perfectly match the random state.
- Usually a small cluster set and small supercell (<50 atoms) is still fine.
- Treating spin-up and spin-down as two different electronic states, SQS can be used to model magnetic disorder with an Ising model.

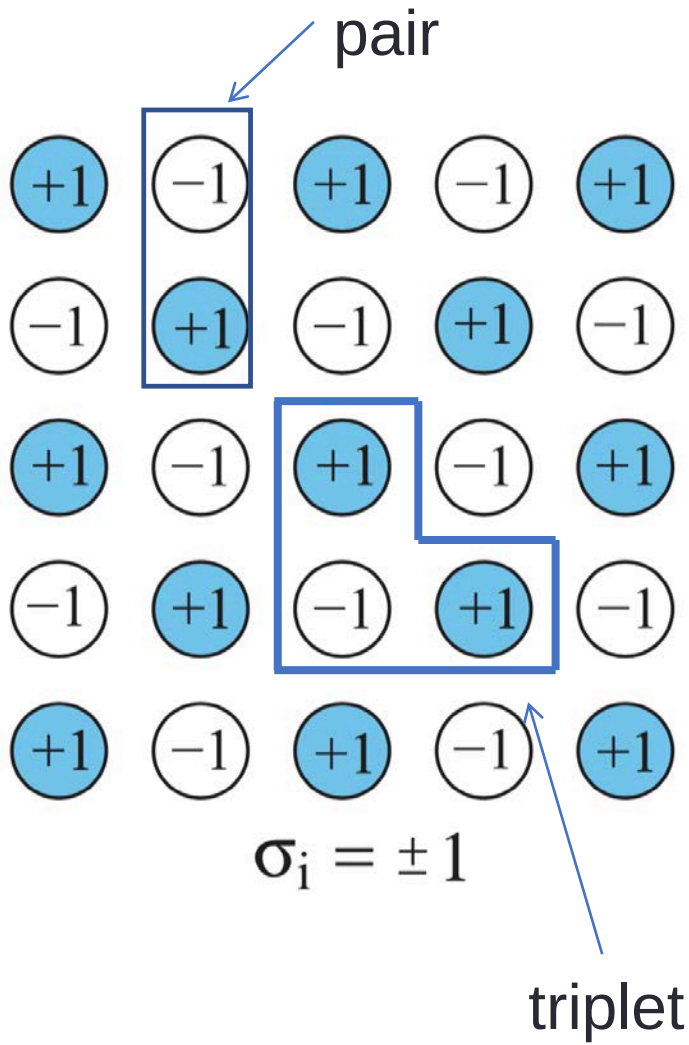

Figure adapted from http://www.brown.edu/Departments/Engineering/Labs/avdw/atat/atattalk.pdf

Computational Methods

Cluster Expansion

- The cluster expansion formalism [1-4] describes an effective representation of the crystalline material system's energy, through a cluster set and their coefficients. Typically, the cluster set need to remain as small as a few pairs and triplets.
- This compact representation is the key to fast ground state search and statistical sampling of microscopic states.
- It is realized in the open source implementation of The Alloy Theoretic Automated Toolkit (ATAT).

[1] van de Walle, A., Asta, M. & Ceder, G. *Calphad-Computer Coupling Phase Diagrams Thermochem.* **26,** 539–553 (2002).
[2] van de Walle, A. *Calphad-Computer Coupling Phase Diagrams Thermochem.* **33,** 266–278 (2009).
[3] van de Walle, A. & Asta, M. *Model. Simul. Mater. Sci. Eng.* **10,** 521–538 (2002).
[4] van de Walle, A. & Ceder, G. *J. Phase Equilibria* **23,** 348–359 (2002).

Cluster Expansion

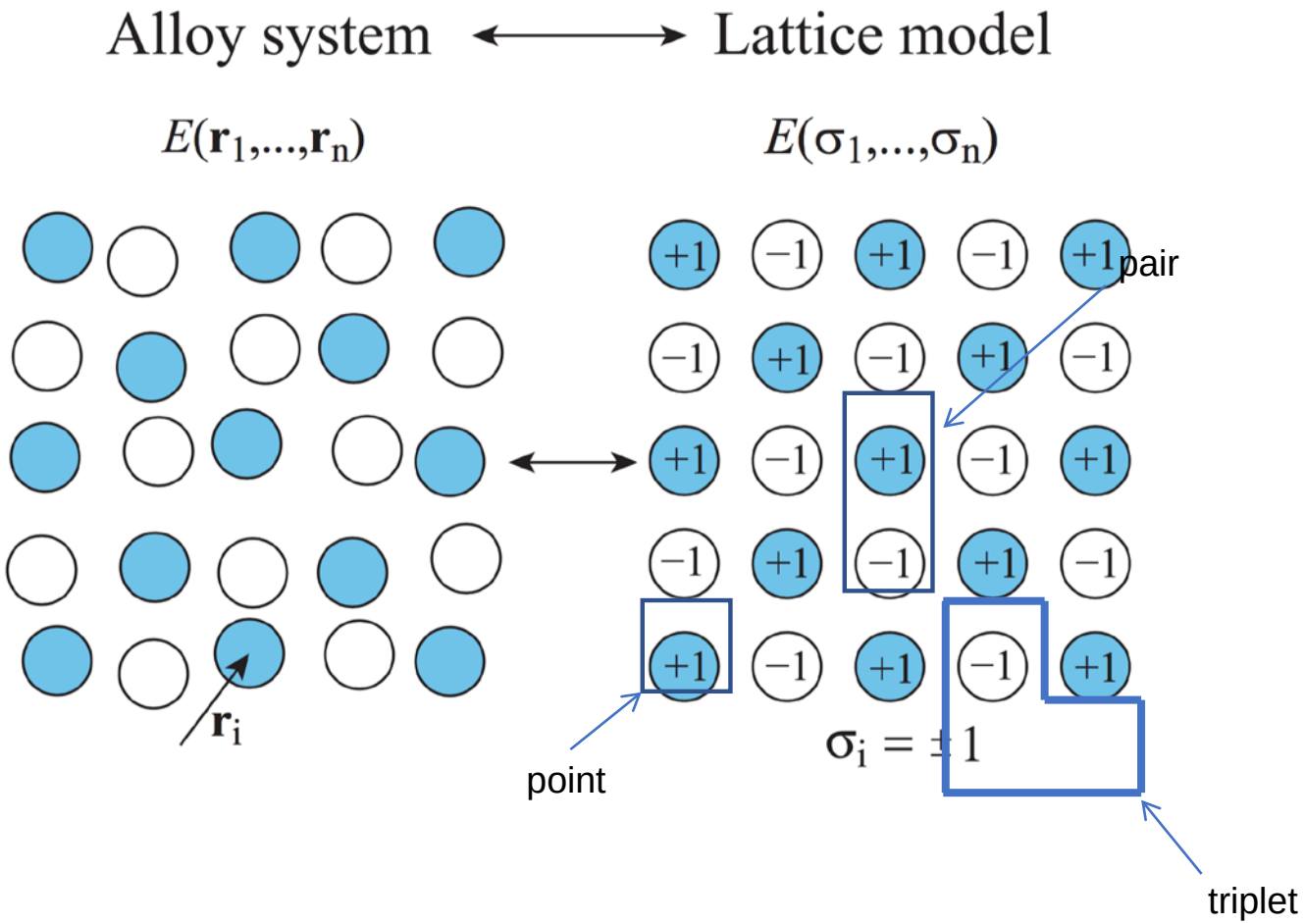

$$E^{(n)}(\sigma) = \sum_{\alpha} J_\alpha \, \sigma_\alpha^{(n)}$$

$$\sigma_\alpha^{(n)} = \prod_{i \in \alpha} \sigma_i^{(n)}$$

Adapted from http://www.brown.edu/Departments/Engineering/Labs/avdw/atat/atattalk.pdf

Cluster Expansion

$$E^{(n)}(\sigma) = \sum_{\alpha} J_\alpha \, \sigma_\alpha^{(n)}$$

$$\sigma_\alpha^{(n)} = \prod_{i \in \alpha} \sigma_i^{(n)}$$

- α is a cluster of a set of substitutional sites (i) of the parent lattice, and each substitutional site is assigned a configuration variable σ_i.
- The sum is taken over all the clusters of the parent lattice
- Coefficients J_α are called effective cluster interactions (ECIs).

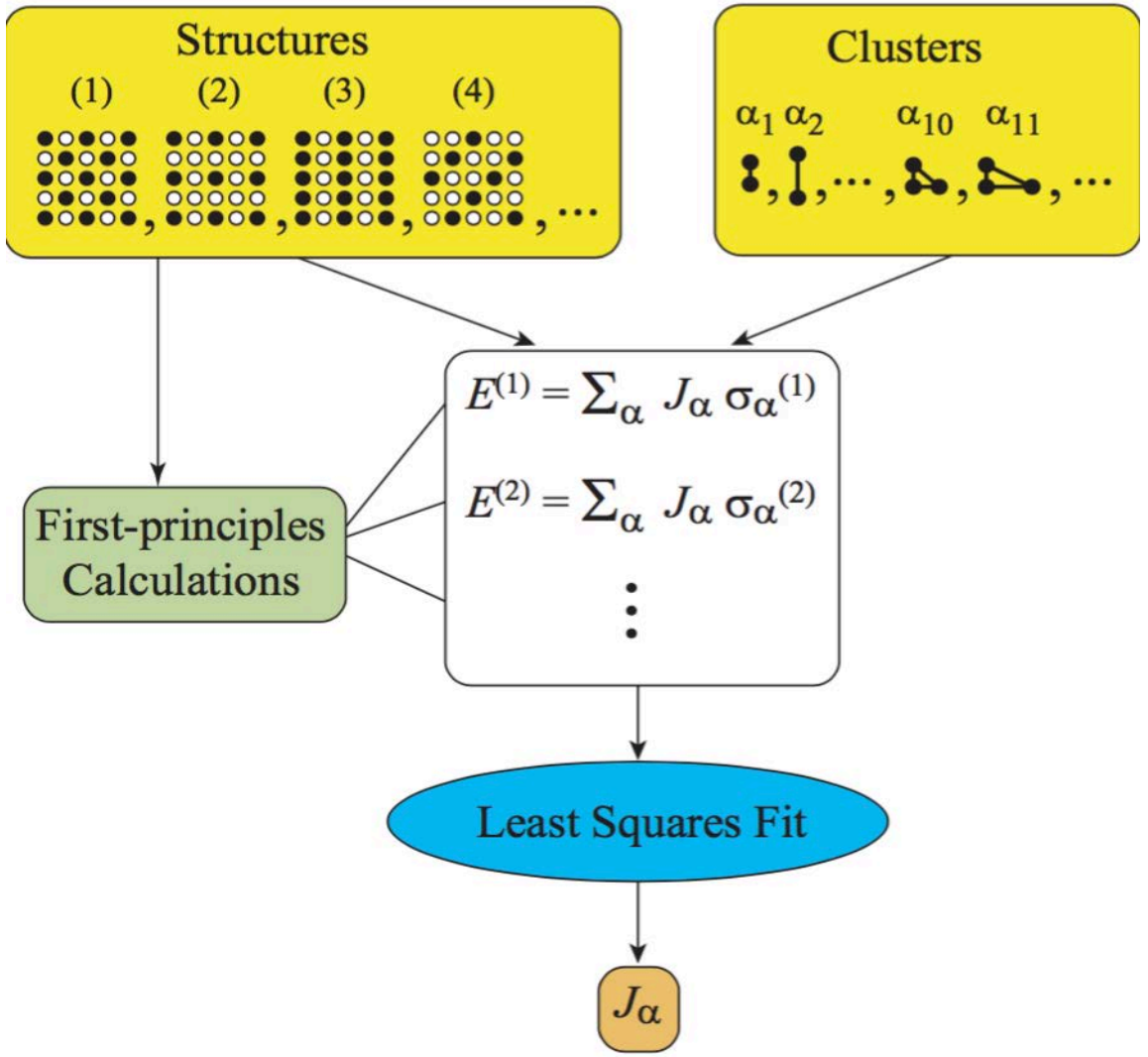

Adapted from http://www.brown.edu/Departments/Engineering/Labs/avdw/atat/atattalk.pdf

- The optimal cluster set and ECIs is selected by minimizing the cross-validation (CV) score,

$$CV = \frac{1}{n}\sum_{i=1}^{n}\left(E_i - \hat{E}_{(i)}\right)^2,$$

where E_i is the first-principles calculated energy of structure i, and $E_{(i)}$ is the "leave-one-out" (without structure i) least-squares fitted energy to prevent over-fitting.

Adapted from http://www.brown.edu/Departments/Engineering/Labs/avdw/atat/atattalk.pdf

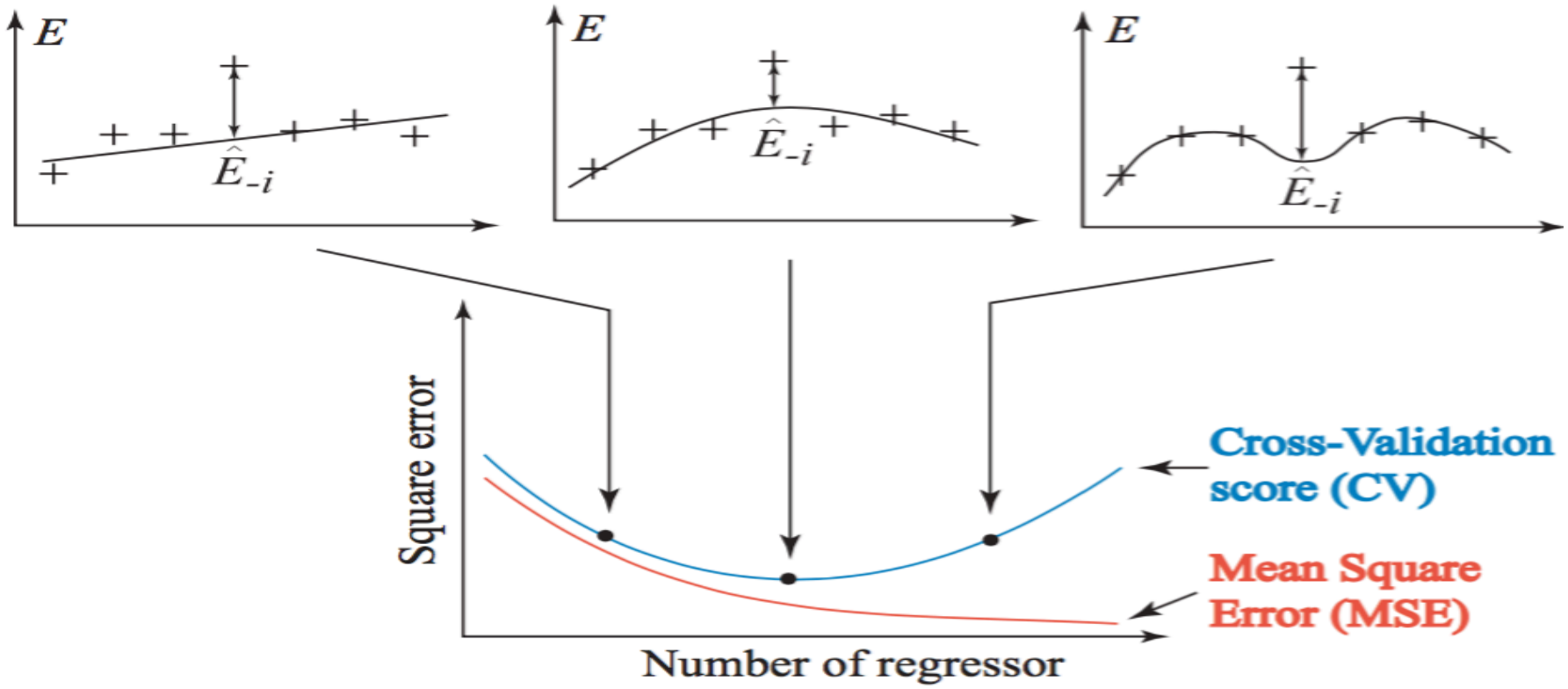

Phase Diagrams: Purely Theoretical

- It calls for an efficient way of generation and energy prediction of tens of thousands of structures consisting of tens of thousands of atoms, beyond the brute force first-principles calculation of each structure. The cluster expansion formalism offers such a solution.

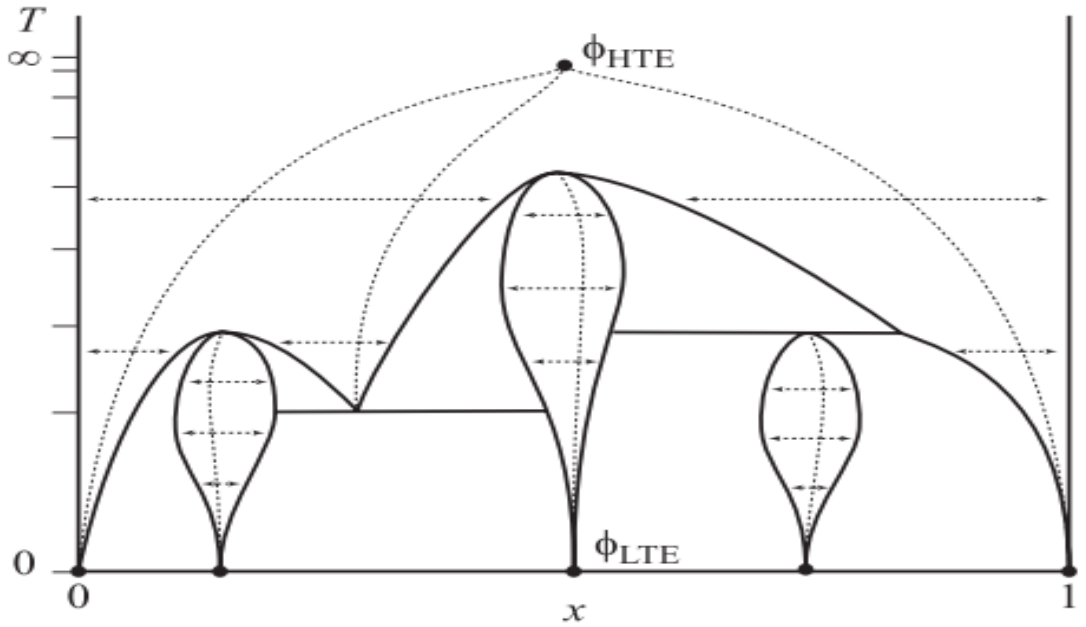

A. van de Walle and M. Asta, *Model. Simul. Mater. Sci. Eng.* **10**, 521 (2002).

Phase Diagrams: Purely Theoretical and Predictive

- *T-x* phase diagrams provide the road maps for synthesis of a particular phase or a mixture at a given set of external conditions.
- Common examples are solids with vacancies, interstitials and substitutions.

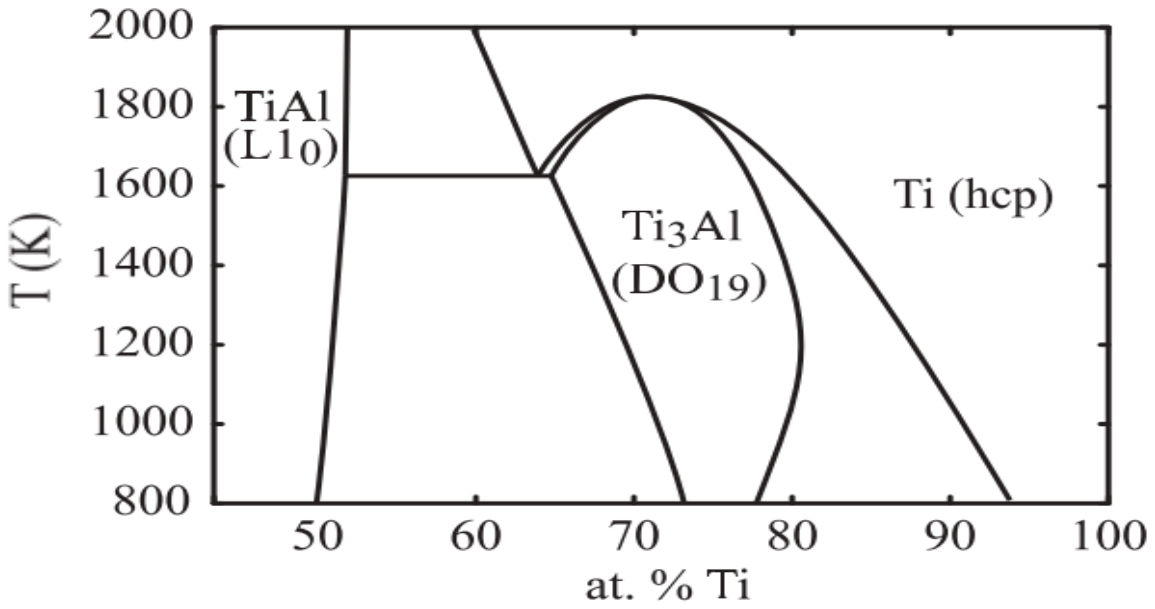

A. van de Walle and M. Asta, *Model. Simul. Mater. Sci. Eng.* **10**, 521 (2002).

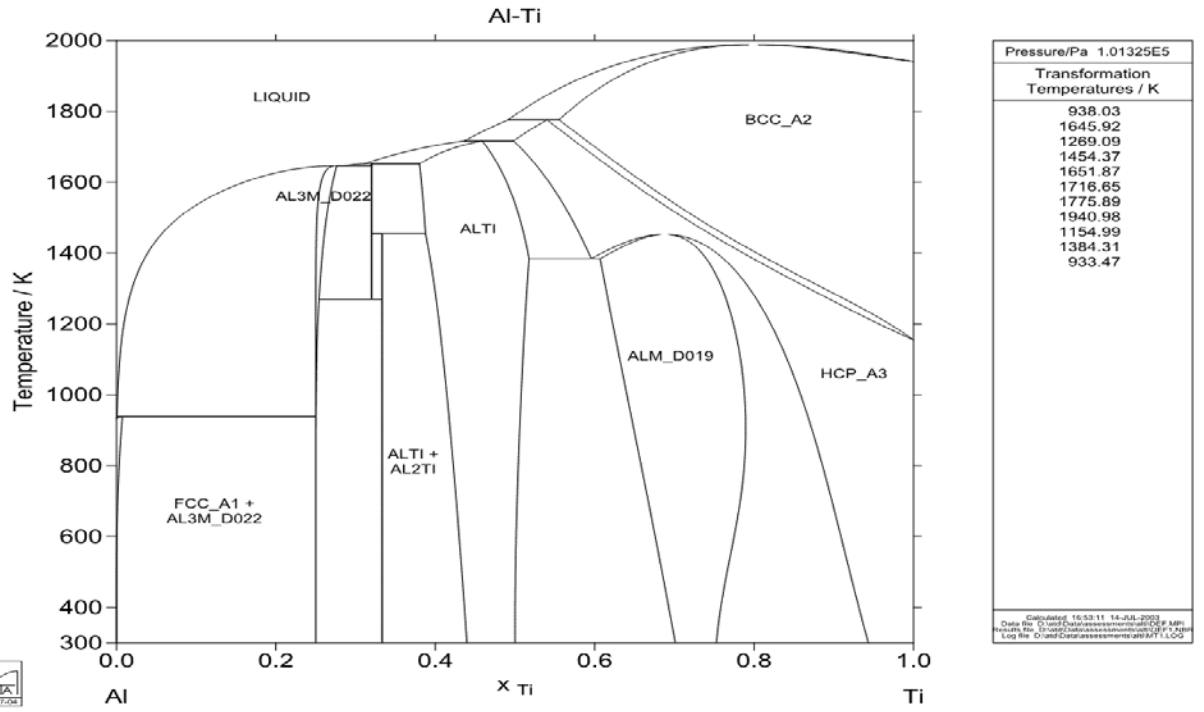

http://resource.npl.co.uk/mtdata/phdiagrams/png/alti.png

Materials of Interest

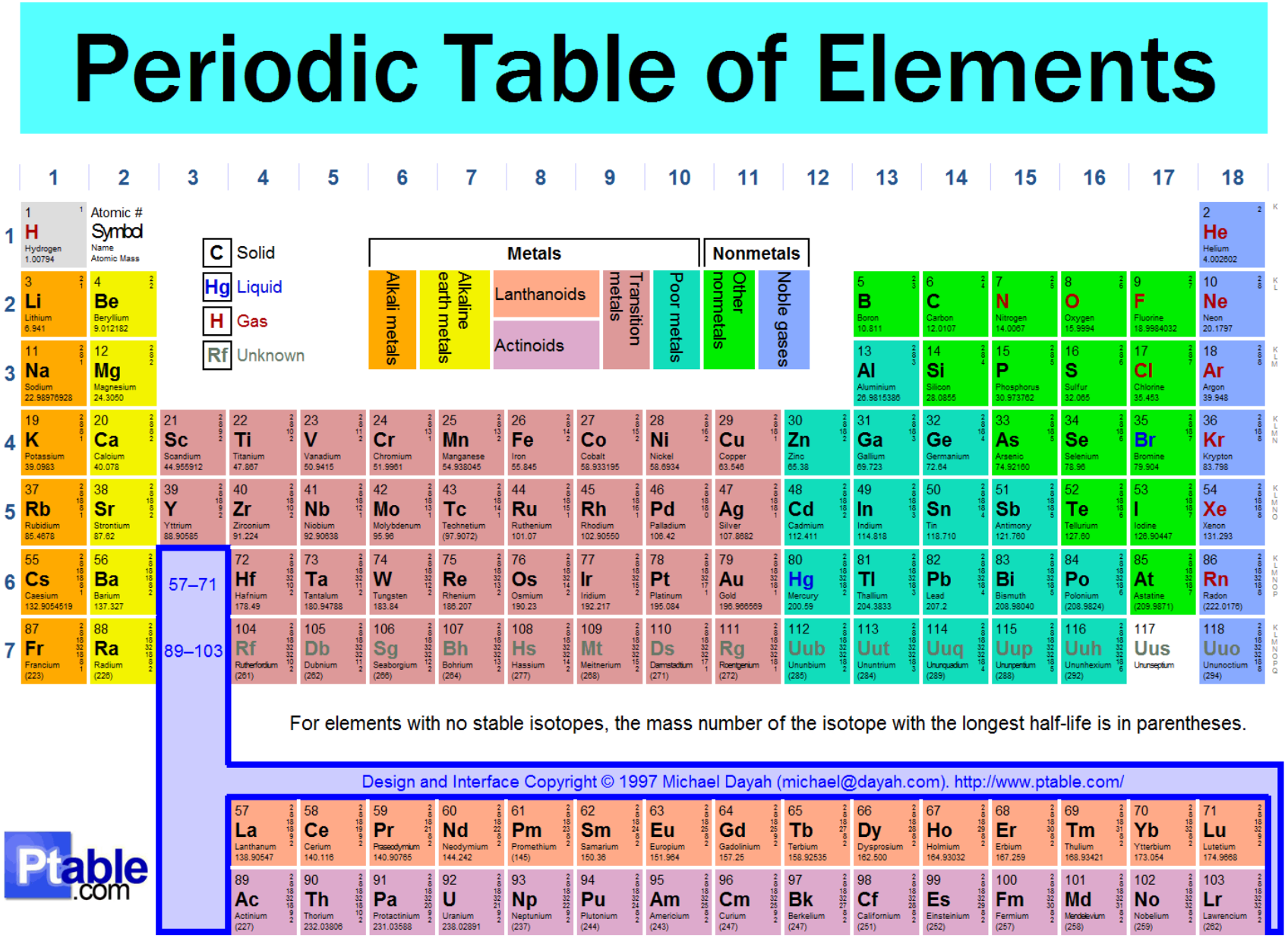

Introduction

- Improved properties achieved by alloying TiN with other transition metals, such as Zr, Hf, V, Nb, Ta, Mo, W.
- Alloying with these elements increases Valence Electron Concentration (VEC) and hence enhances ductility and toughness coupled with **decreased hardness**.
- Jhi and Ihm [1, 2] showed that **hardness can be increased** by decreasing the VEC when N is replaced with C in the TiC_xN_{1-x} system.
- Holleck [3] indicated that the hardness of carbonitrides is maximized at a VEC = 8.4 electrons/f.u.
- TiN-AlN alloys have shown enhanced hardness but have low maximum operating temperature and phase decomposition [4-6].
- We propose alloying TiN with Sc and Y to enhance hardness by lowering VEC.

[1] S.H. Jhi, S.G. Louie, M.L. Cohen, J. Ihm, Phys. Rev. Lett. 86 (2001) 3348–3351, http://dx.doi.org/10.1103/PhysRevLett.86.3348.
[2] S.H. Jhi, J. Ihm, S.G. Louie, M.L. Cohen, Nature 399 (1999) 132–134, http:// dx.doi.org/10.1038/20148.
[3] H. Holleck, Material selection for hard coatings, J. Vac. Sci. Technol. A Vacuum, Surfaces, Film 4 (1986) 2661, http://dx.doi.org/10.1116/1.573700.
[4] Bivas Saha, Samantha K. Lawrence, Jeremy L. Schroeder, Jens Birch, David F. Bahr, and Timothy D. Sands,
[5] Sit Kerdsongpanya, Björn Alling, and Per Eklund, J. Appl. Phys. 114, 073512 (2013); https://doi.org/10.1063/1.4818415
[6] Per Eklund, Sit Kerdsongpanya and Bjo¨rn Alling, Journal of Materials Chemistry C, 4(18) · February 2016 DOI: 10.1039/c5tc03891j

Results: Properties of End Members

- Lattice constants, Hardness (H_V) agree values from experiments.
- End members have high hardness: TiN (23.4), ScN (**25.1)**, and YN (20.6) in GPa.
- Volumes/f.u.: TiN (19.2), ScN (23.11) and YN (29.53) in $Å^3$
- Volumes linked directly to the ionic radii of corresponding transition metals.
- [(Ti^{4+} (0.61 Å), Sc^{3+} (0.75 Å) and Y^{3+} (0.9 Å)*]
- High C_{44} (shear-resistant) means high Vickers hardness (H_V).
- Small volume → High density → Higher hardness.

*Shannon R D, Acta Crystallogr. A 32 751–67, 1976.

Results: Properties of End Members

End members	a (Å)	V/f. u. (Å^3)	C_{11} (GPa)	C_{12} (GPa)	C_{44} (GPa)	B (GPa)	G (GPa)	k	ν	E (GPa)	H_V (GPa)
TiN	4.25 4.245[a] 4.21[e]	19.19 19.1[b]	582.2	122.6	158.9	275.8 318[b,h] 303[i] 267[j] 290[k] 280[l]	184.2	0.67	0.23	452.1 590[c]	23.4 20.2[f] 21[g]
ScN	4.52 4.501[d] 4.52[e]	23.11	389.5	104.2	166.8	199.3 182 ± 40[d]	156.7	0.79	0.19	372.5 388 ± 20[d]	25.1 24.4 ± 1.3[d]
YN	4.91	29.53	318.5	76.8	122.6	157.4	121.9	0.77	0.19	290.7	20.6
Intermetallics	Lattice Type	V/ N (Å^3)	$\overline{C}_{11}$ (GPa)	$\overline{C}_{12}$ (GPa)	$\overline{C}_{44}$ (GPa)	B (GPa)	G (GPa)	k	ν	E (GPa)	H_V (GPa)
$TiScN_2$	Rhombohedral	20.57	483.4	135.4	186.5	251.4	181.4	0.72	0.21	438.7	25.2
$TiSc_8N_9$	Hexagonal	22.14	440.7	112.5	164.7	221.9	164.5	0.74	0.2	395.6	24.3
$TiSc_9N_{10}$	Triclinic	22.21	444	104.3	168.6	217.5	169.1	0.78	0.19	402.8	26.1
$Ti_3Sc_2N_5$	Monoclinic	20.51	488.6	125.1	190.5	246.3	186.9	0.76	0.2	447.6	27.3

- Lattice constants, Hardness (H_V) agree values from experiments.
- End members have good hardness TiN: 23.4., ScN: **25.1**, and YN: 20.6 in GPa.
- High C_{44} (shear-resistant) means high Vickers hardness (H_V).

Results

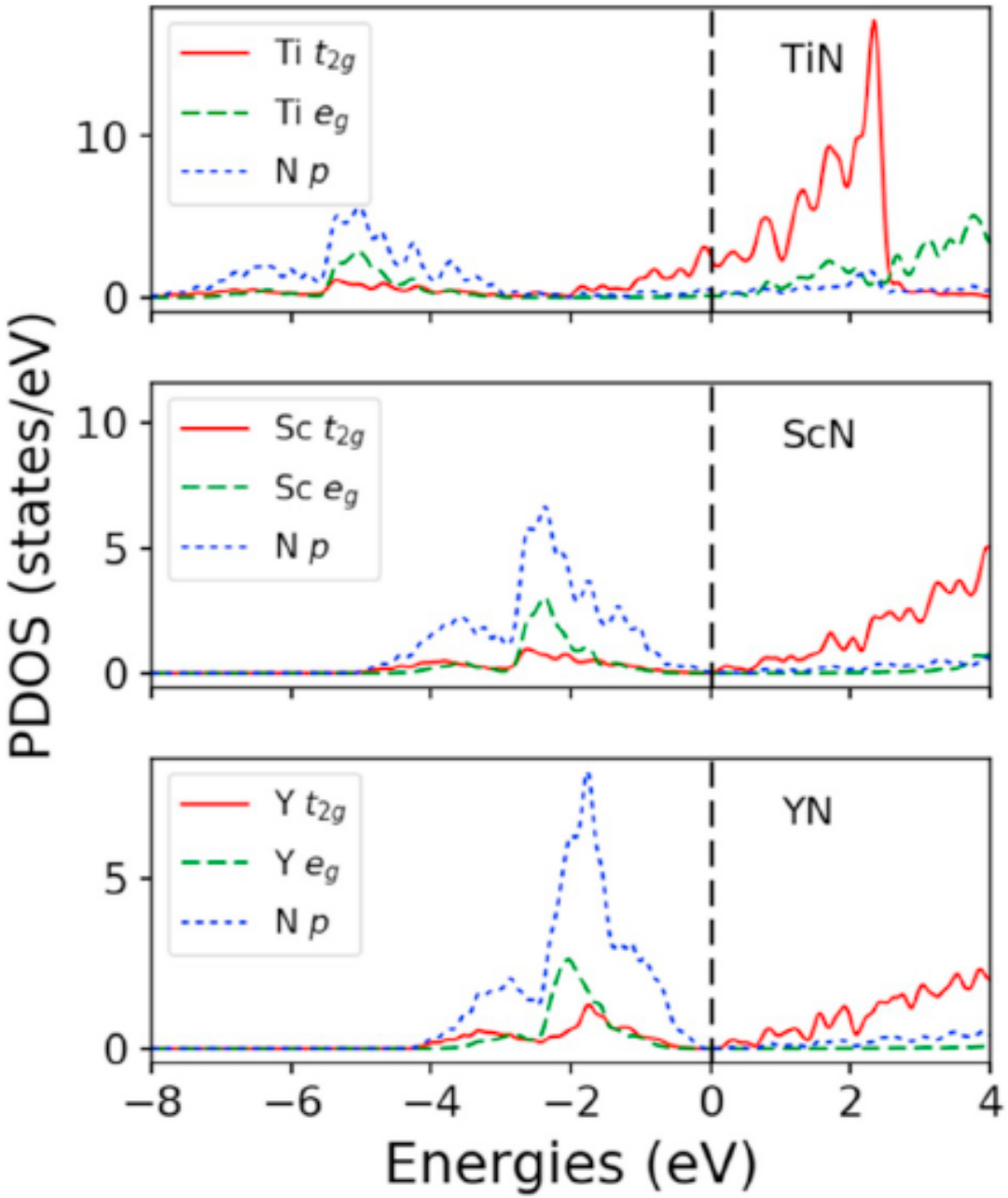

Properties of End members: TiN, ScN and YN

High hardness is attributed to:

- High occupation of bonding e_g orbitals
- Favors M d – N p hybridization at low energies

(Occupied e_g: strongly resistant to shearing and compression)

- Low occupation of antibonding t_{2g} state

(Occupied t_{2g} favor shearing due to enhanced second-nearest neighbor metal interactions)

TiN is metallic while ScN and YN are very small band gap semiconductors (≈0.9 eV) due to strongly localized 3d orbitals.

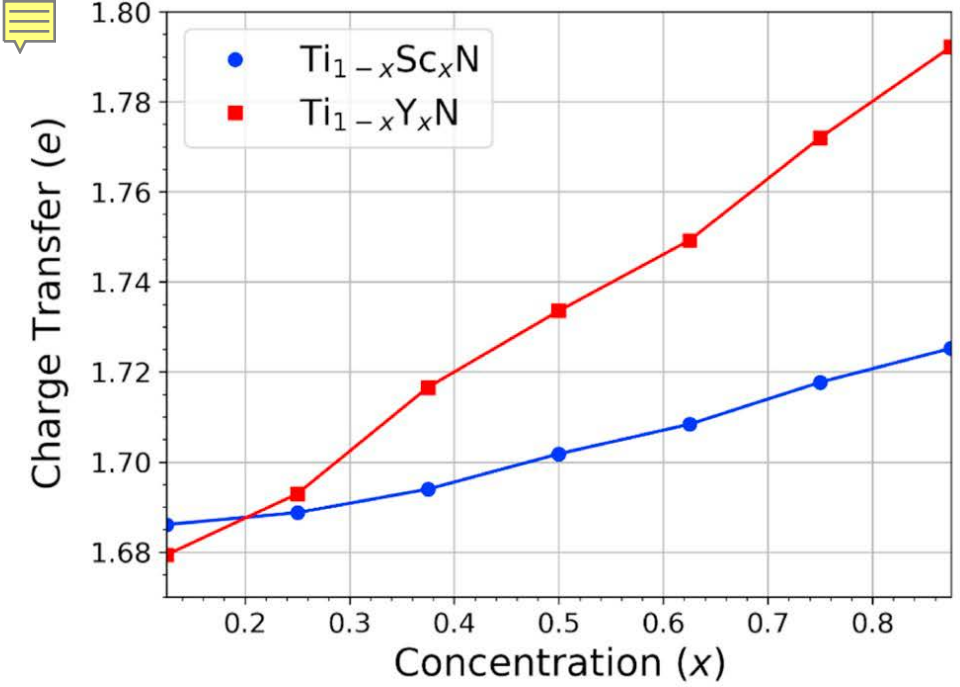

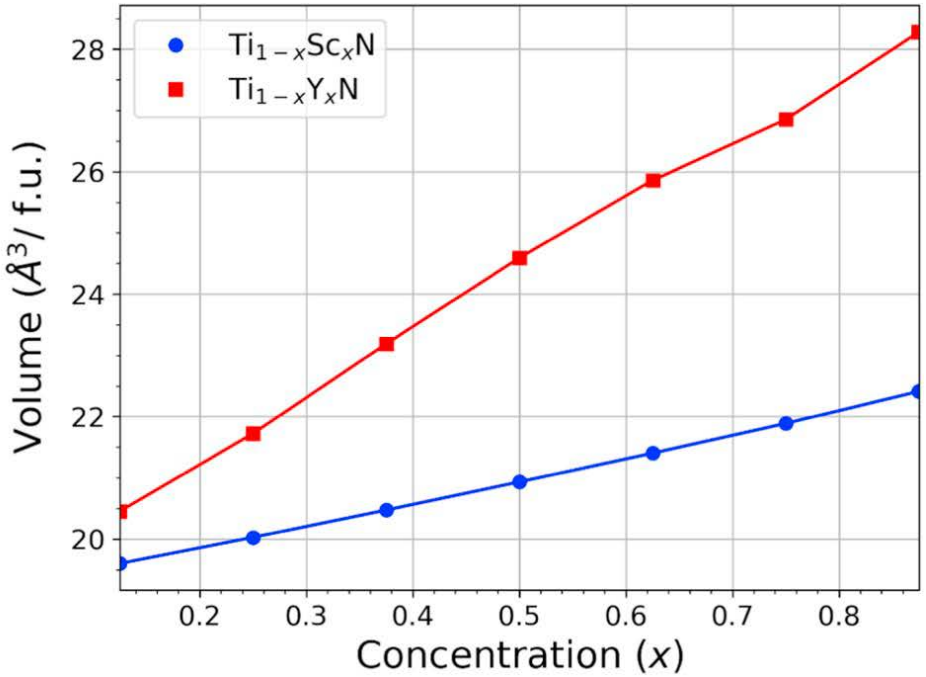

Results: Lattice Similarity and Mismatch

- Lattice Mismatch: Differences in Size, Ionic radius, electronegativity

- Ionic radii: [Ti^{4+} (0.61 Å), Sc^{3+} (0.75 Å) and Y^{3+} (0.9 Å)] [1]
- Electronegativity: Ti (1.32), Sc (1.20), and Y (1.11) [2]

- Large diff in electronegativities & Ionic radii
  → Greater charge transfer
  → Substantial volume change
  → Positive strain energy and structural distortion.

- Charge transferred per atom ΔZ_Y, = (1.2) (1-c_Y) ($\Delta\phi$) [3]

[1] R.D. Shannon, Revised effective ionic radii and systematic studies of interatomic distances in halides and chalcogenides, Acta Crystallogr. A 32 (1976) 751–767
[2] A.L. Allred, E.G. Rochow, J. Lnorg. Nucl. Chem. 5 (1958) 264–268, https://doi.org/10.1016/0022-1902(58)80003-2
[3] A. R. Miedema, Journal of Less-Common Metals, 32 (1973) 117-136 (https://doi.org/10.1016/0022-5088(73)90078-7))

Results: Energy landscapes

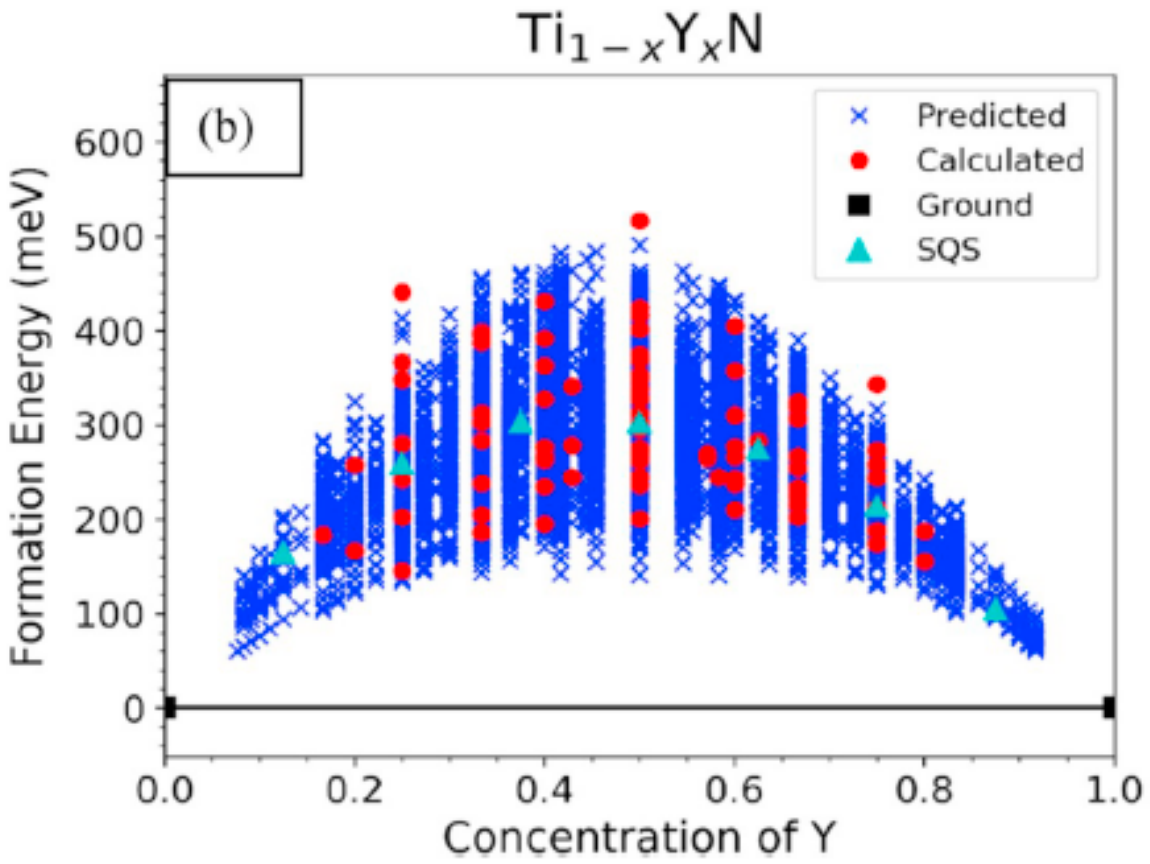

$Ti_{1-x}Y_xN$ System

- Strongly endothermic mixing: Upward bowing in ΔE_f (reaching as high as 500 meV/atom)
- Attributed to large lattice mismatch between TiN and YN, causing structural distortions and positive strain energy
- End Members are the only stable ground states in $Ti_{1-x}Y_xN$ solid solution.

Results: Phase diagrams

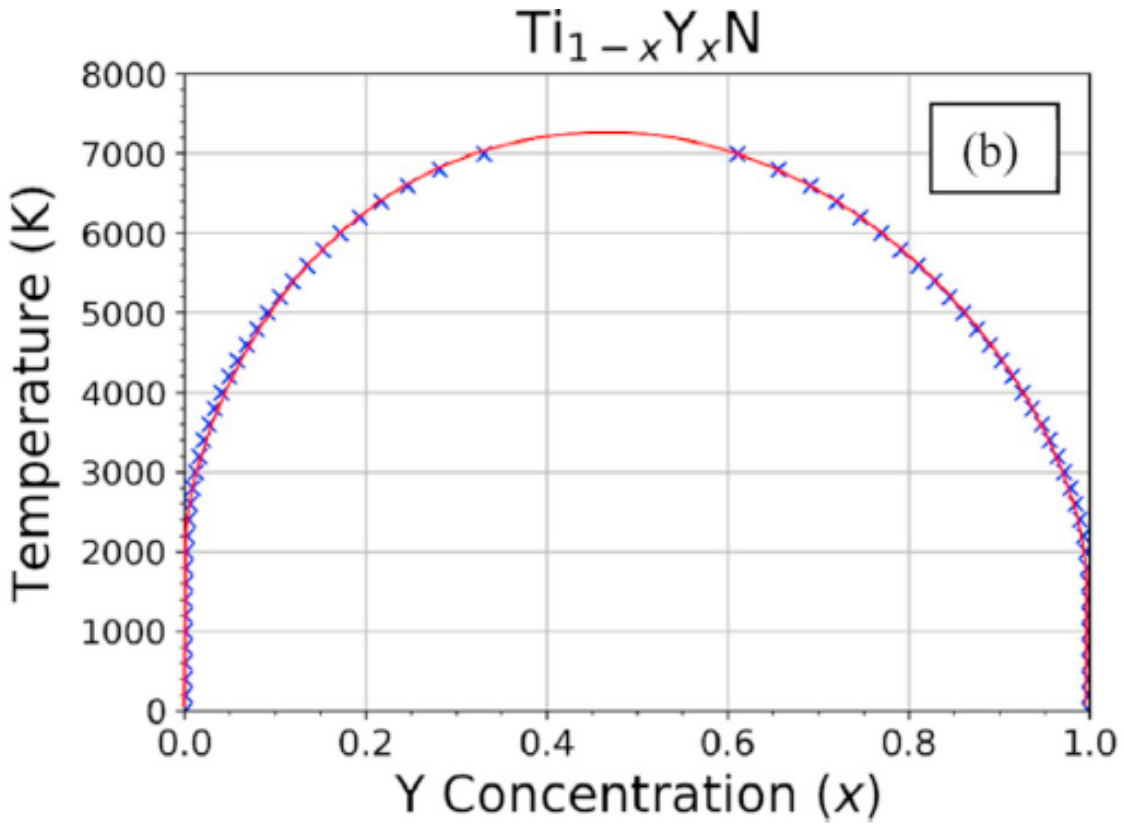

$Ti_{1-x}Y_xN$: Miscibility gap far above the room temp & (T_c) = 7225 K.

- Alloying is recommended only at low or high concentrations, where configurational entropy dominates.
- In such cases, Y can diffuse into grain boundaries and enhances oxidation resistance and mechanical properties.
- Provides opportunities to engineer hard coatings with segregated concentration variations as reported by Lewis et al. [1] and Choi et al. [2].

[1] D.B. Lewis, L.A. Donohue, M. Lembke, W.D. Munz, R. Kuzel, V. Valvoda, C.J. Blomfield, The influence of the yttrium content on the structure and properties of Ti1-x-y-zAlxCryYzN PVD hard coatings, Surf. Coat. Technol. 114 (1999), 187.
[2] W.S. Choi, S.K. Hwang, C.M. Lee, Microstructure and chemical state of Ti1-xYxN film deposited by reactive magnetron sputtering, J. Vac. Sci. Technol. A 18 (2000) 2914, https://doi.org/10.1116/1.1319680.

Results: Energy landscapes

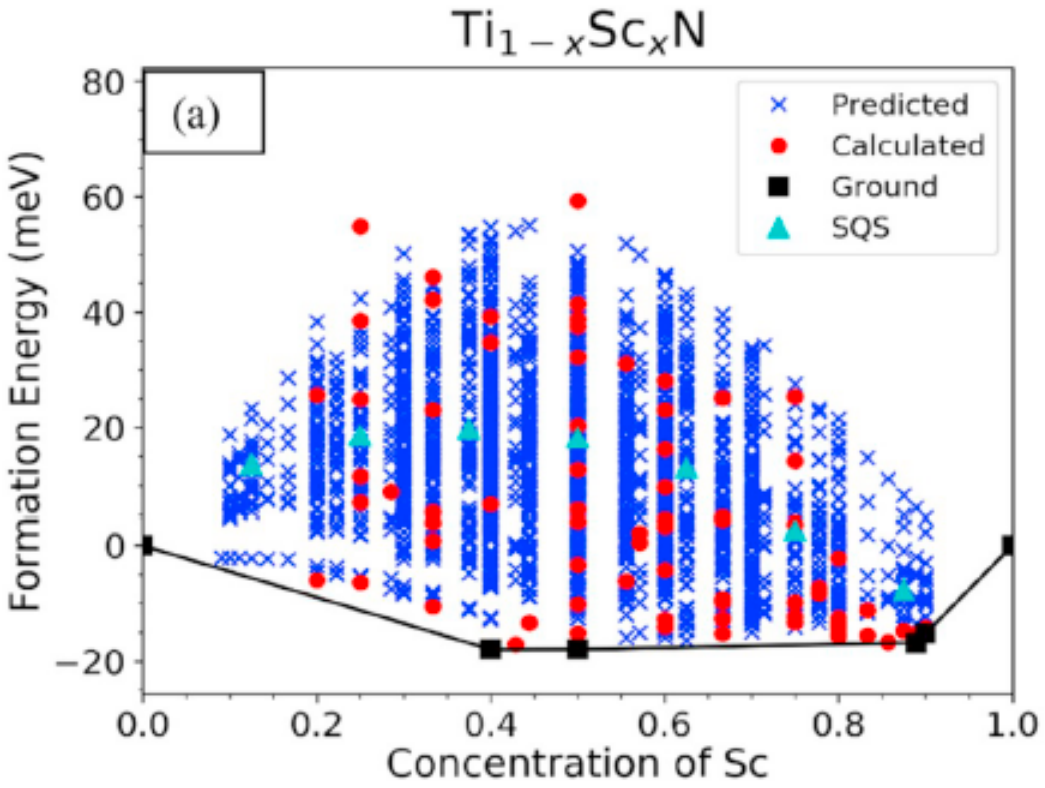

$Ti_{1-x}Sc_xN$ System

- Small differences in ionic radii and electronegativity alloying only minor changes in charge transfer and volumes.
- Exothermic mixing of TiN and ScN: downward bowing in ΔE_f
- Effect of chemical bonding controlled by changes in valency to lower the energy of the system.
- Decrease in ΔE_f at intermediate concentrations.
- Four novel ground states lie on the convex hull: $TiScN_2$, $TiSc_8N_9$, $TiSc_9N_{10}$, and $Ti_3Sc_2N_5$
- Thermodynamically Stable: Formation energies are -17.968, -16.832, -15.264 and -17.987 meV respectively.

Results: Phase diagrams

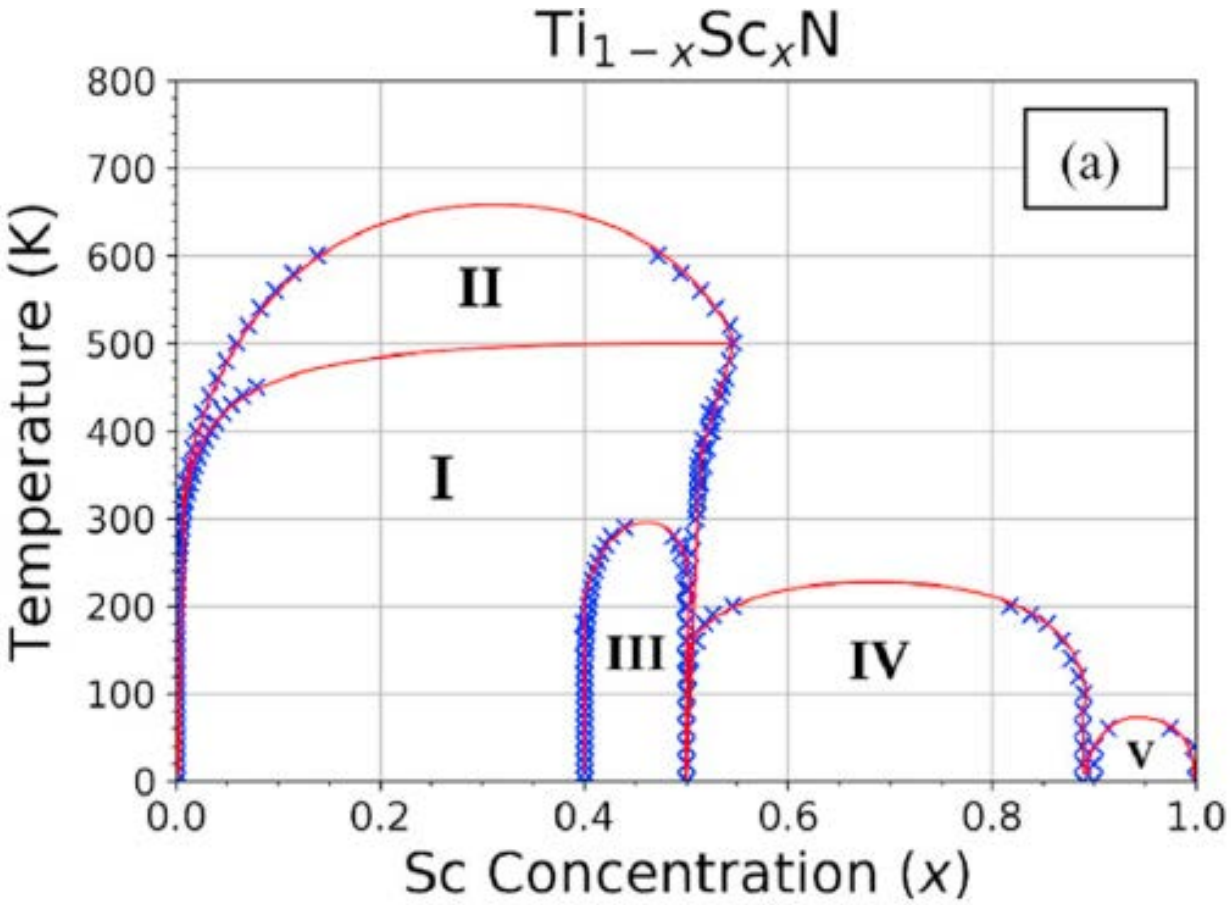

$Ti_{1-x}Sc_xN$

- Upper consolute temperature T_c **: 660 K,** above which a complete miscibility occurs.
- 5 major intermetallic phases representing stability of heterogeneous mixture

Results

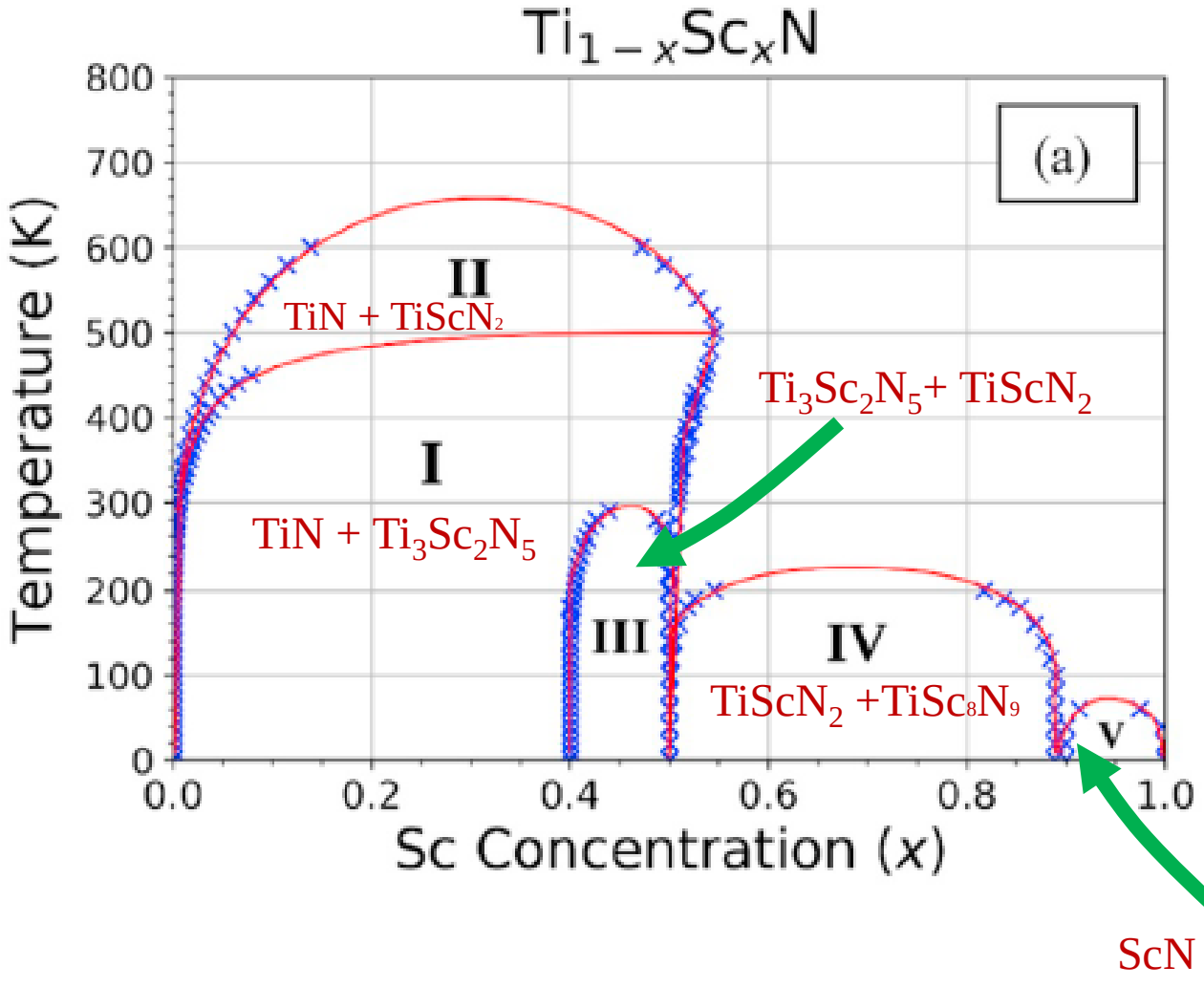

5 major intermetallic phases representing stability of heterogeneous mixture in **$Ti_{1-x}Sc_xN$**

660 K: complete miscibility achieved for all Sc concentration

Region I: TiN + $Ti_3Sc_2N_5$ (0 – 50% Sc, 0 K – 500K)

Region II: TiN + $TiScN_2$ (0 – 50% Sc, 500 K – 660K)

Region III: $Ti_3Sc_2N_5$ + $TiScN_2$ (40 – 50% Sc, Moderately low temp up to 300K)

Region IV: $TiScN_2$ + $TiSc_8N_9$ (50 – 90% Sc, 225 K)

Region V: TiS_9cN_{10} + ScN (90 – 100% Sc, miscibility at 65 K)

Results: Phase diagrams

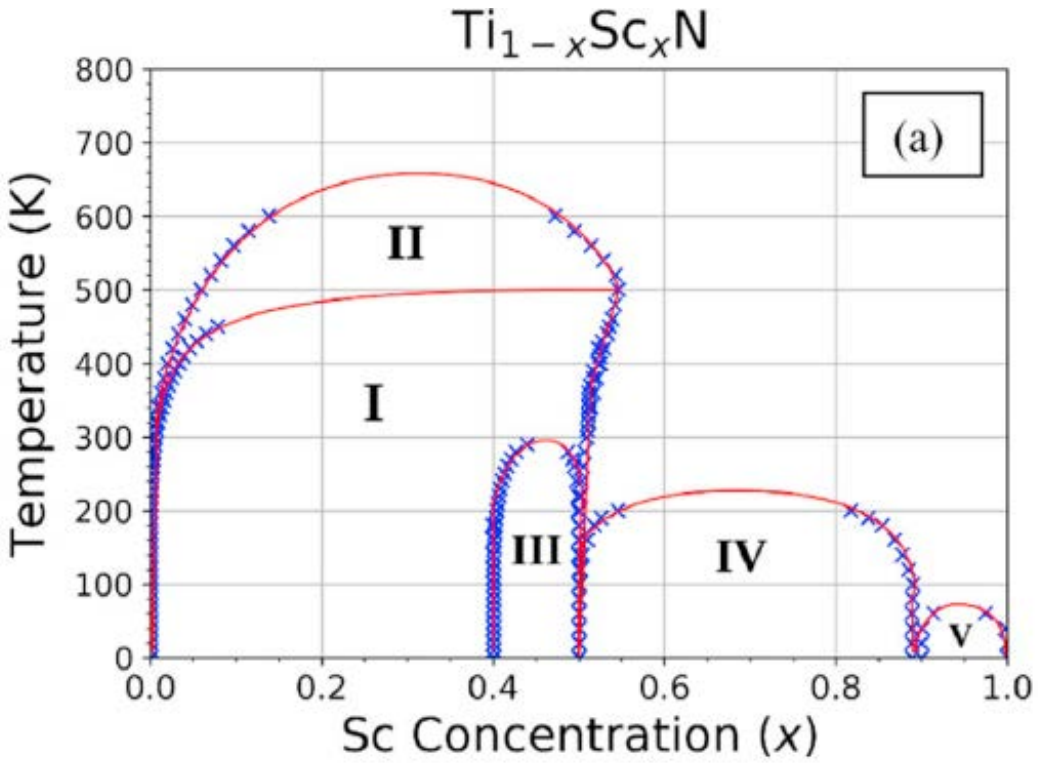

- $Ti_3Sc_2N_5$ Covers a significant portion in Phase diagram showing strong stability
  - Region I: TiN + $Ti_3Sc_2N_5$ (0 – 50% Sc, 0 K – 500K)
  - Region II: TiN + $TiScN_2$ (500 K - 660K)
  - Region III: $Ti_3Sc_2N_5$ + $TiScN_2$ Moderately low temp up to 300K
  - Region IV: $TiScN_2$ + $TiSc_8N_9$ (225 K)
  - Region V: $TiSc_9N_{10}$ + ScN (miscibility at 65 K)
- Previous work of Kerdsongpanya *et al.* , where $Sc_{1-x}Ti_xN$ changes from ordered to disordered solid solution at x = 0.5 at 1073 K (first principles) [1]
- Gall *et al.* Synthesized $Ti_{1-x}Sc_xN$ epitaxial layers at 750 °C by reactive magnetron sputtering [2]

[1] Sit Kerdsongpanya, Björn Alling, and Per Eklund, J. Appl. Phys. 114, 073512 (2013); https://doi.org/10.1063/1.4818415]
[2] D. Gall, M. Stoehr, and J. E. Greene, PHYSICAL REVIEW B, VOLUME 64, 174302 (2001), DOI: 10.1103/PhysRevB.64.174302

Results

Properties of TiN-ScN intermediate phases

- Predicted novel intermetallics: $TiScN_2$, $TiSc_8N_9$, $TiSc_9N_{10}$, $Ti_3Sc_2N_5$
- Thermodynamically stable due to low formation energy, mechanically stable
- Crystallize in rhombohedral, hexagonal, triclinic, and monoclinic symmetries
- Preserve the rocksalt-type lattice ordering of parent lattice.
- High hardness: 24.3 to 27.3 Gpa
- $Ti_3Sc_2N_5$ is the hardest (27.3 GPa)
- $Ti_3Sc_2N_5$ stable through a wide range of Sc concentration (from 0 to 50% and up to 500 K)

Results

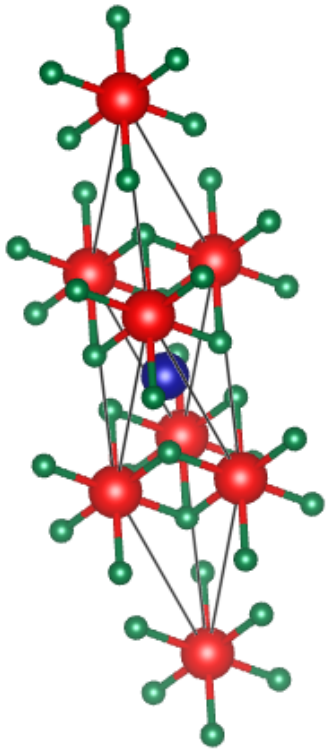

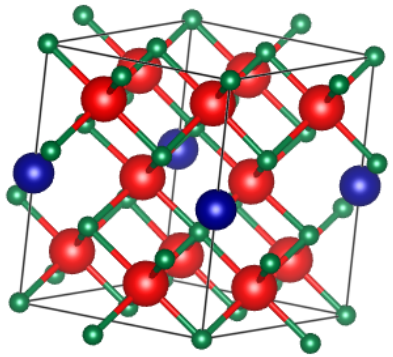

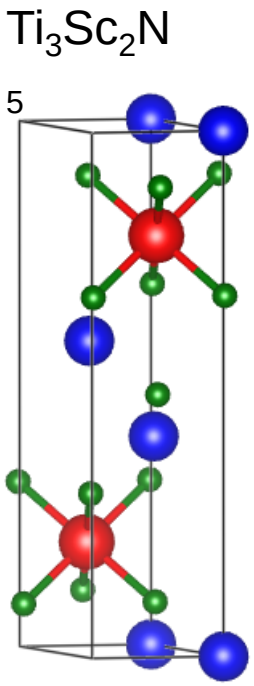

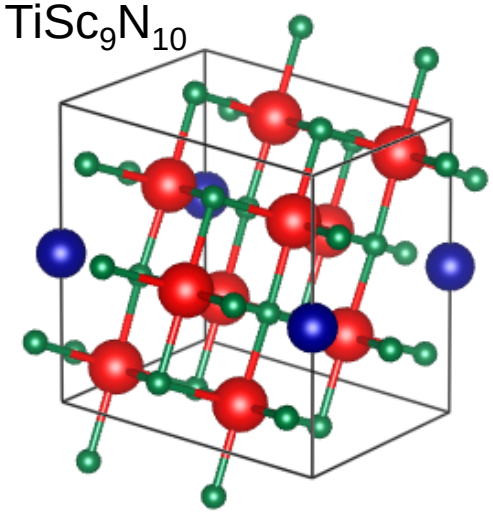

Properties of TiN-ScN intermediate phases

New ground states preserve the layered rocksalt-type lattice of parent end members.

Hardest $Ti_3Sc_2N_5$ (27.3 Gpa)
Exceeds the hardness of end members.

Highest H_V at Valence Electron Concentration (VEC) = 8.6

Figure: Computed Conventional Unit Cell of novel intermetallics. Blue, red and green spheres represent Ti, Sc and N atoms respectively.

Results

Structure of TiN-ScN intermetallic phases

Predicted Ground States	Lattice - Type	Space Group and Number	Lattice Parameter
$TiScN_2$	Rhombohedral	$R\bar{3}m$ (166)	a = b = c = 5.35 Å α = β = γ = 33.32°
$TiSc_8N_9$	Hexagonal	$P\bar{3}1m$ (162)	a = b = 5.46 Å, c = 7.72 Å α = β = 90°, γ = 120°
$TiSc_9N_{10}$	Triclinic	$P\bar{1}$ (2)	a = 5.46 Å, b = 6.31 Å, c = 7.06 Å, α = 102.91°, β = 97.39° γ=106.83°
$Ti_3Sc_2N_5$	Monoclinic	C2/m (12)	a = b = 3.07 Å, c = 12.69 Å α = 90.00°, β = 83.02°, γ = 60.00°

Although deviated from cubic symmetry due to mixing enthalpy, new ground states preserve the layered rocksalt-type lattice ordering and octahedral ligand of parent end members.

Results

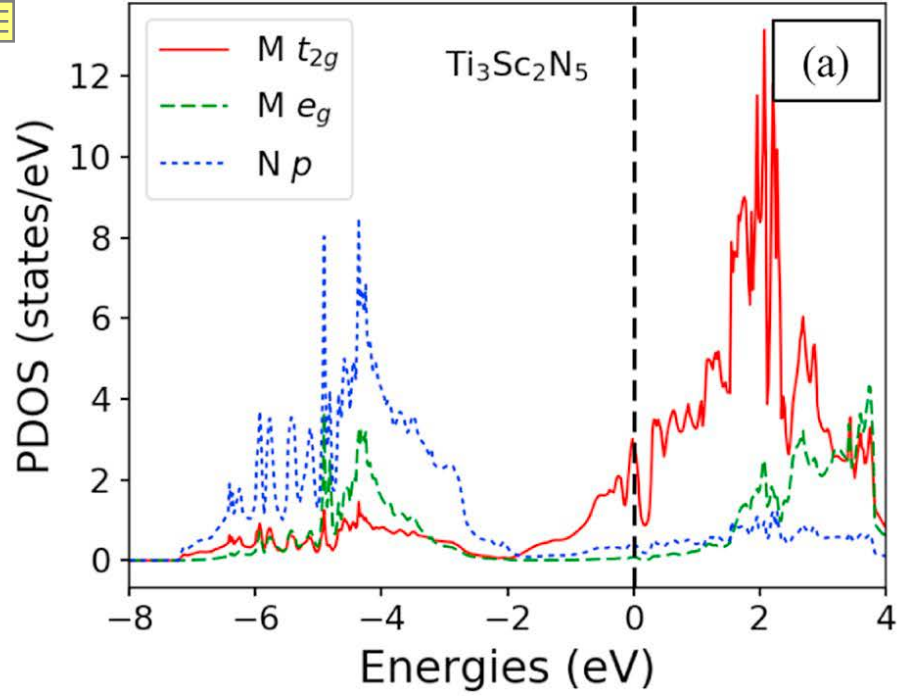

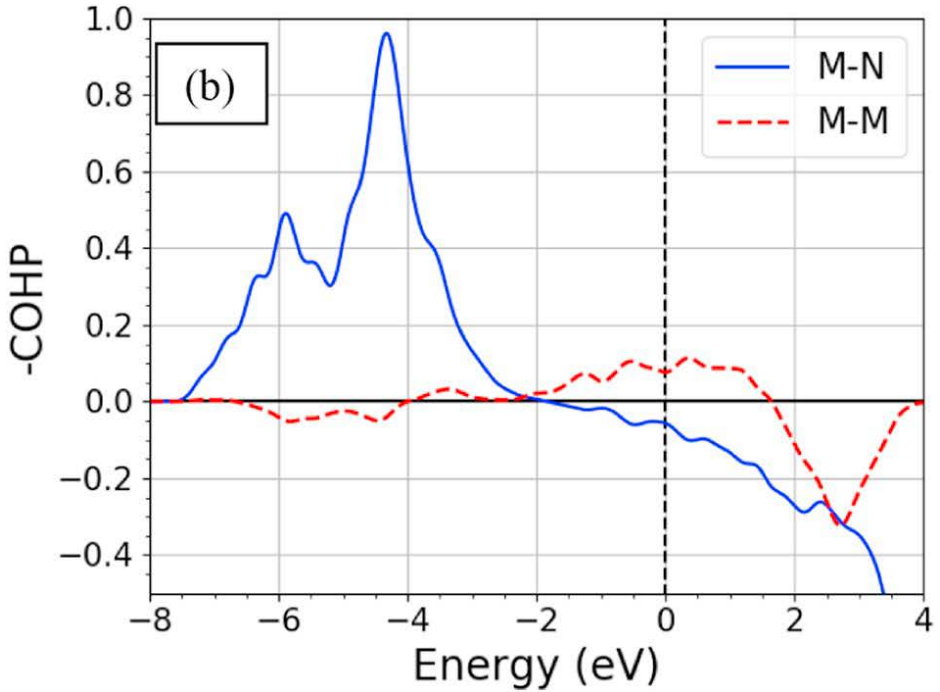

TiN-ScN intermediate phases

High hardness of $Ti_3Sc_2N_5$: PDOS and COHP curve

- Strong d-p hybridization for -7 eV to -2 eV
- COHP curve: Complete occupation of the M-N bonding states
- Greater covalent character.
- Decreased occupation of metal t_{2g} orbitals, owing to the VEC of $Ti_3Sc_2N_5$ (8.6) being less than TiN (9).
- Lowest volume and highest density among the intermetallics contribute further to the hardness.

Results

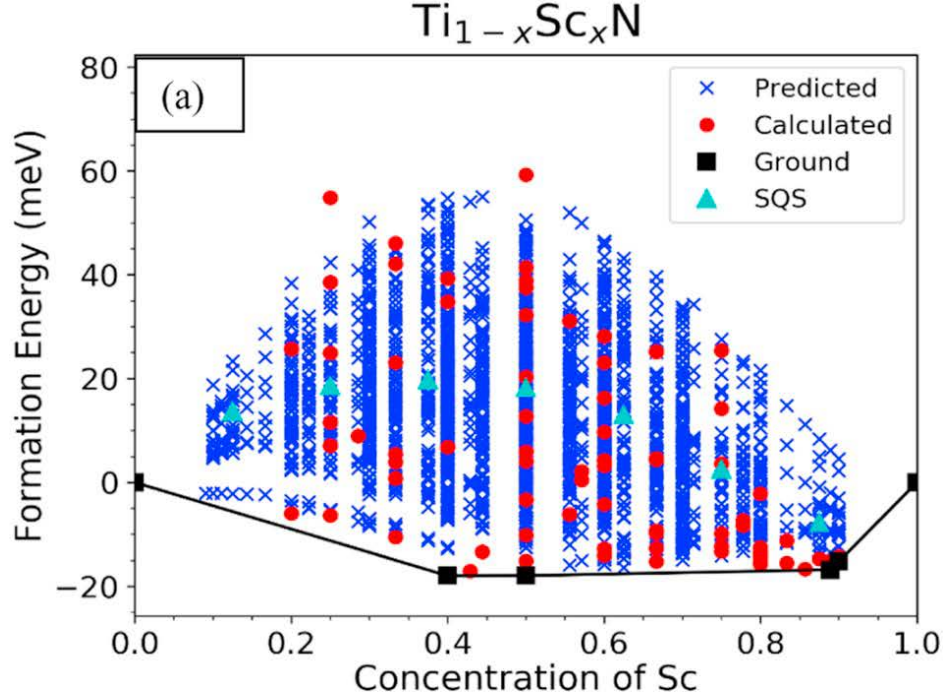

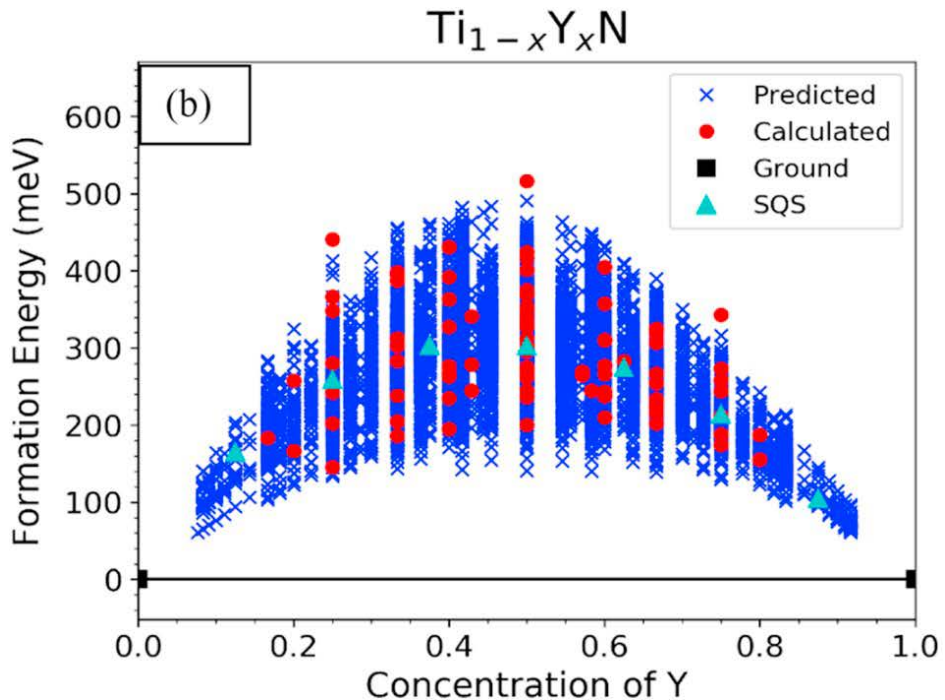

Effects of cation disorder

- SQSs: Represented by Cyan triangles in the energy landscapes.
- SQSs of $Ti_{1-x}Y_xN$: Upward bowing in formation energies.
- High Tc: large and unfavorable difference between the ΔE_f of the SQSs at intermediate concentration to those of end members.
- SQSs of $Ti_{1-x}Sc_xN$: Not much difference in ΔE_f of SQSs and ground states (upto 30 to 10 meV from intermediate to high SC concentration)
- This resulted to lower T_c from 65 K to 660 K.

Results

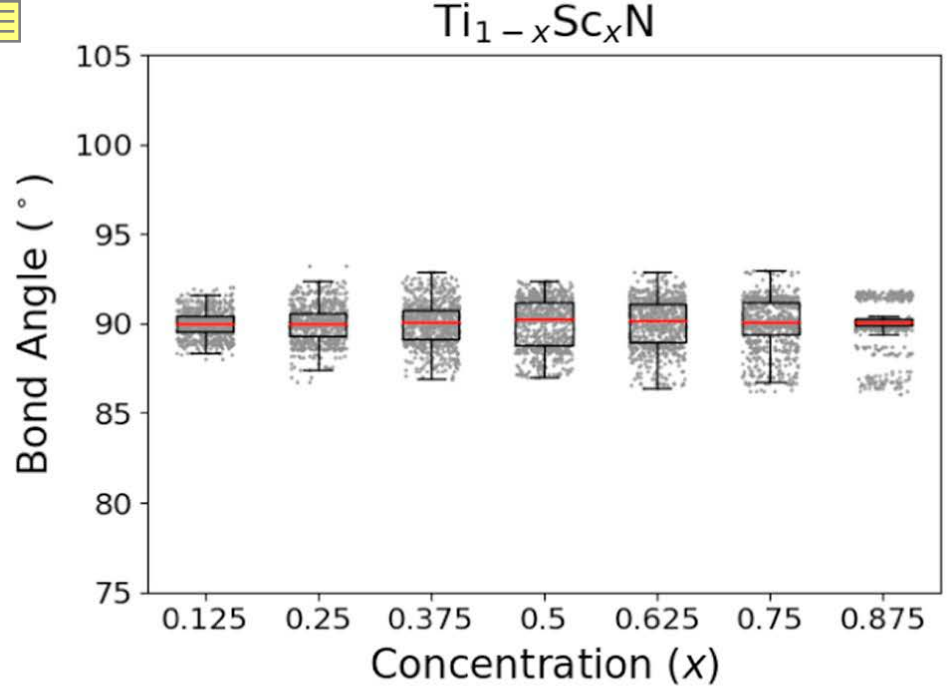

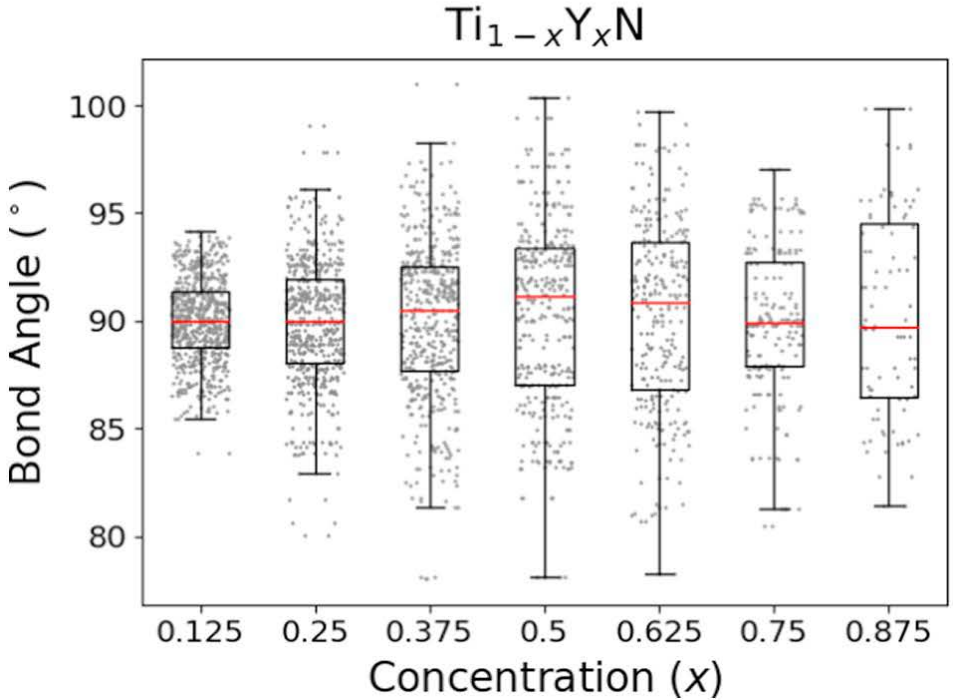

Effects of cation disorder

- Cation disordering causes atomic displacements within local octahedral environment.
- In $Ti_{1-x}Y_xN$,distortions are large with variations in bond angles by up to 20 degrees.
-
- In $Ti_{1-x}Sc_xN$, only minor variation in bond angle as high as 8 degrees.
- Lattice mismatch between Ti and Y and similarity between Ti and Sc plays important roles.

Results

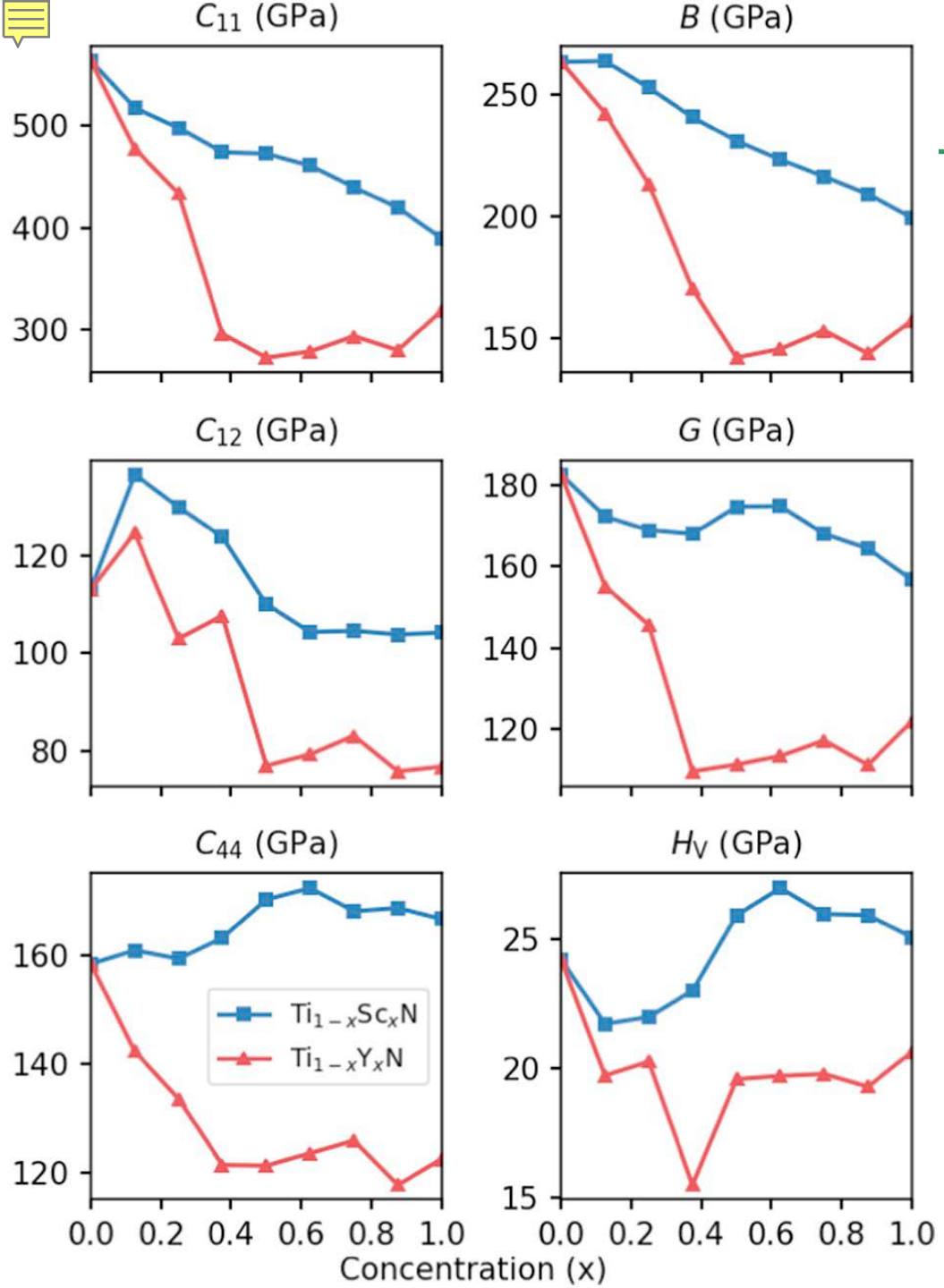

Mechanical properties of SQSs

- C_{11} and C_{12} decrease with Sc and Y concentration due to volume expansion.
- High C_{44} means high H_V.
- Significant enhancement in the hardness in $Ti_{1-x}Sc_xN$ but not in $Ti_{1-x}Y_xN$.
- High H_V of 27 GPa at x = 0.625 in In $Ti_{1-x}Sc_xN$. (VEC = 8.4)
- Agrees well with the work by Holleck [1]: Maximized hardness of titanium carbo-nitrides at VEC = 8.4
- Ordered phase $Ti_3Sc_2N_5$, H_V =27.3 GPa at VEC = 8.6.

[1] Holleck, Material selection for hard coatings, J. Vac. Sci. Technol. A Vacuum, Surfaces, Film 4 (1986) 2661, http://dx.doi.org/10.1116/1.573700.

Results

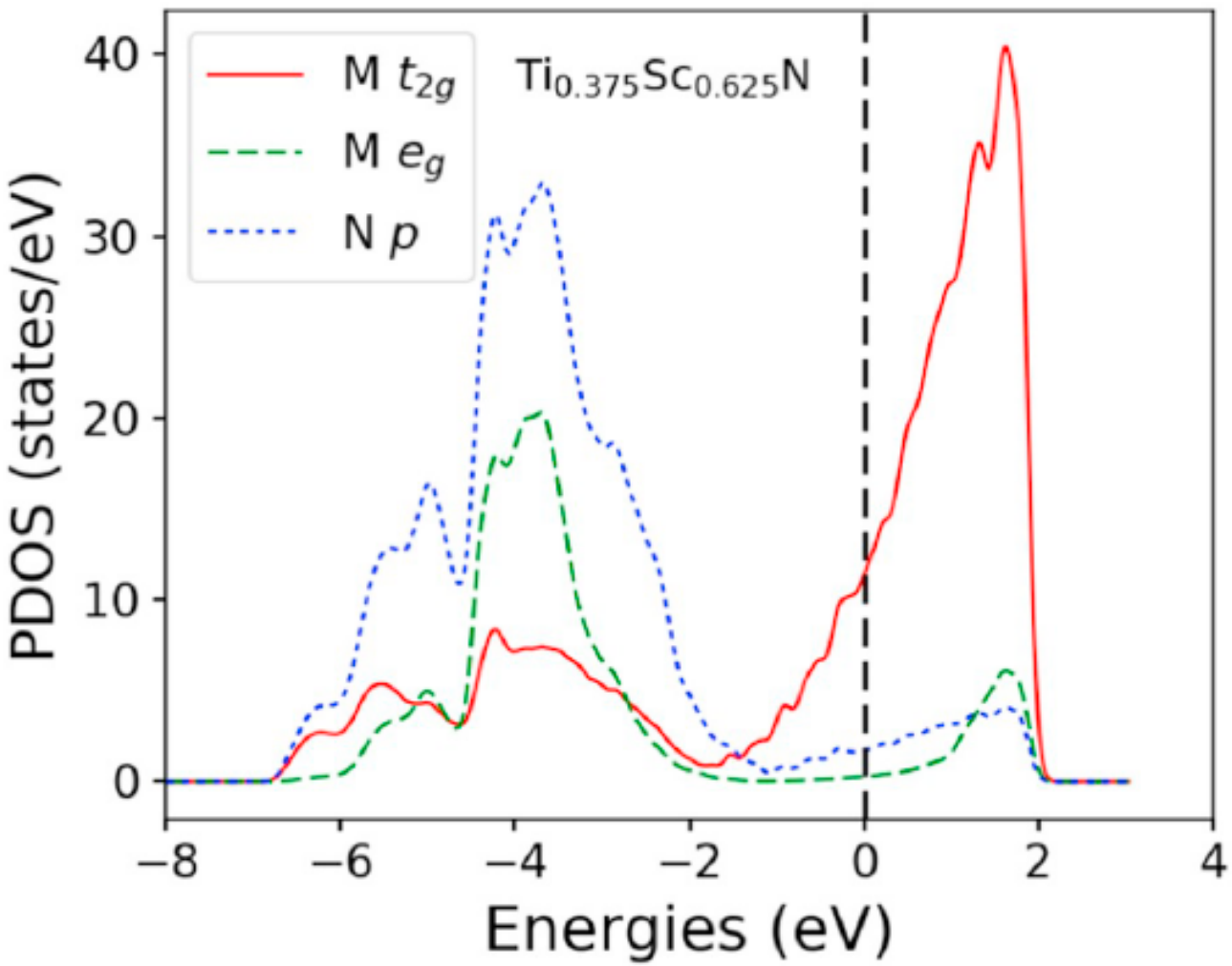

Maximum hardness also extends to the case of random solid solution.

At x = 0.625 atomic Sc concentration, H_V = 27 GPa, VEC = 8.4.

Attributed to the M-N bonding states due to increased occupancy of metal e_g states.

Conclusion

- Investigated the phase stability of two quasi-binary ceramic systems, $Ti_{1-x}Sc_xN$ and $Ti_{1-x}Y_xN$ ($0 \leq x \leq 1$) using DFT, CE, and MC simulations.
- Exothermic mixing in $Ti_{1-x}Sc_xN$ yielded 4 novel stable intermetallic: $TiScN_2$, $TiSc_8N_9$, $TiSc_9N_{10}$, and $Ti_3Sc_2N_5$.
- $Ti_{1-x}Y_xN$ shows strong endothermic mixing due to the large lattice mismatch between Ti and Y, hence solubility is achieved only at very high temp (>7220 K).
- End members TiN, ScN and YN exhibit H_V of 24.2, 25.1, and 20.6 GPa respectively.
- $Ti_3Sc_2N_5$ achieves the highest hardness of 27.3 Gpa at VEC = 8.6.
- Random solid solution of $Ti_{1-x}Sc_xN$ exhibits hardness of 27 GPa at x =0.625 and VEC = 8.4

Conclusion

- $Ti_{1-x}Sc_xN$ alloys exhibit enhanced hardness and stability due to strong *d-p* hybridization of metal-nitrogen orbitals and minimal volume expansion attributed to similarity in cation properties of Ti and Sc.
- $Ti_{1-x}Y_xN$ alloys only useful for hardness enhancement by diffusing through grain boundaries in TiN.
- The $Ti_{1-x}Sc_xN$ alloys make them promising candidates for improved hard coating applications.
- We recommend mechanical properties tuning by controlled VEC for structural and functional alloys.

Thank you!

Tian's Equation for calculating H_V (Vicker's Hardness)

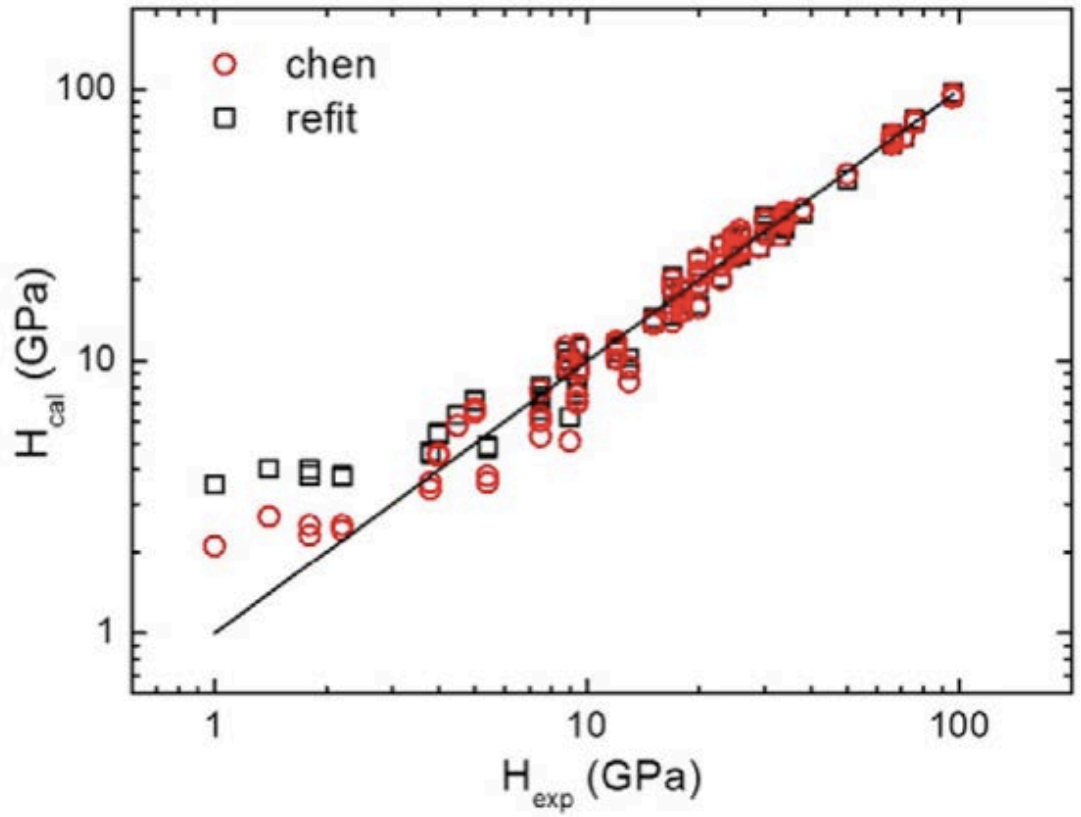

$$B = (C_{11} + 2C_{12})/3$$

$$G_v = [(C_{11} - C_{12}) + 3C_{44}]/5$$

$$G_R = [5(C_{11} - C_{12})C_{44}]/(4C_{44} + 3C_{11} - 3C_{12})$$

$$G = G_{VRH} = (G_v + G_R)/2$$

$$k = G/B$$

$$H_V = 0.92k^{1.137}G^{0.708}$$

Y. Tian *et al.*, Int. J. Refract. Met. Hard Mater. **33**, 93 (2012).

Concentration (x), elastic constants (C_{11}, C_{12}, C_{44}), Bulk modulus (B), Shear modulus (G), Pugh's ratio (k), Poisson's ratio (v), Young's modulus (E) and Vickers hardness (H_V) of the SQS of $Ti_{1-x}Y_xN$.

SQSs	Concentration (x)	C_{11} (GPa)	C_{12} (GPa)	C_{44} (GPa)	B (GPa)	G (GPa)	k	v	E (GPa)	H_V (GPa)
$Ti_{1x}Sc_xN$	0	563.2	113.1	158.6	263.1	182.5	0.69	0.22	444.7	24.2
	0.125	517.3	136.5	161.1	263.5	172.2	0.65	0.23	424.2	21.7
	0.25	497.6	129.9	159.5	252.4	168.8	0.67	0.23	414.2	22
	0.375	473.7	123.7	163.3	240.4	167.9	0.7	0.22	408.6	23
	0.5	472.2	110	170.4	230.7	174.6	0.76	0.2	418.3	25.9
	0.625	460.6	104.3	172.5	223.1	174.7	0.78	0.19	415.7	27
	0.75	439.5	104.6	168.2	216.2	167.9	0.78	0.19	400.2	26
	0.875	419.3	103.8	168.8	209	164.3	0.79	0.19	390.6	25.9
	1	389.5	104.2	166.8	199.3	156.7	0.79	0.19	372.5	25.1
$Ti_{1-x}Y_xN$	0	563.2	113.1	158.6	263.1	182.5	0.69	0.22	444.7	24.2
	0.125	477.2	124.6	142.5	242.1	155.2	0.64	0.24	383.5	19.7
	0.25	433.4	103	133.7	213.1	145.5	0.68	0.22	355.6	20.3
	0.375	295.7	107.7	121.6	170.3	109.7	0.64	0.23	270.9	15.5
	0.5	272.5	77	121.4	142.2	111.3	0.78	0.19	264.8	19.6
	0.625	278.5	79.3	123.7	145.7	113.4	0.78	0.19	270.2	19.7
	0.75	293.5	83.1	126	153.2	117.2	0.77	0.2	280.2	19.8
	0.875	279.7	75.8	117.9	143.8	111.2	0.77	0.19	265.3	19.3
	1	318.5	76.8	122.6	157.4	121.9	0.77	0.19	290.7	20.6

Numbers of structures calculated with DFT, numbers of clusters in pairs, triplets and quadruplets, and cross-validation (CV) score of $Ti_{1-x}Sc_xN$ and $Ti_{1-x}Y_xN$.

Alloys	Num. of structures	Num. of clusters (pair + trip + quad)	CV Score (meV)
$Ti_{1-x}Sc_xN$	83	15+2+3	4.04
$Ti_{1-x}Y_xN$	91	16+12+16	19.3

(IpCOHP) for different bonding states (Metal: Metal and Metal: Nitrogen) for the three end members and four predicted novel ground states.

Compound	M-N –IpCOHP	M-M -IpCOHP
TiN	1.415	0.137
ScN	1.428	0.012
YN	2.420	0.009
TiScN	1.408	0.043
$Ti_3Sc_2N_5$	1.721	0.078
$TiSc_8N_9$	1.255	-0.008
$TiSc_9N_{10}$	1.228	-0.009

Calculation Parameters

We performed *ab initio* DFT computations using the Vienna Abinitio Simulation Package (VASP) with the projector-augmented wave method (PAW) and Purdew–Burke–Ernzerhoff (PBE) generalized gradient approximation (GGA). We selected the potentials of Ti_sv, Zr_sv, Hf_pv and N, where "_sv" denotes that the semi-core s and p electrons are also included, while "_pv" specifies the semi-core p electrons. The plane wave energy cutoff was chosen to be 520 eV to ensure correct cell volume and shape relaxations. The k-point meshes were created with k-points per reciprocal atom (KPPRA) of 4000. Methfessel-Paxton order 1 smearing was used with a sigma value as small as 0.1 eV. The convergence criterion was set to 10^{-5} eV in energy during the electronic iterations. For structural optimization, the cell volume, shape and atomic positions were allowed to relax until stress was minimized and forces on any atom were below 0.02 eV/Å.

Published work: Z.T.Y. Liu, B.P. Burton, S. V Khare, and D. Gall, *J. Phys. Condens. Matter* **29**, 35401 (2017).

Calculation Parameters

Phase diagrams were generated for $Ti_{1-x}Zr_xN$, $Ti_{1-x}Hf_xN$ and $Zr_{1-x}Hf_xN$ using the Alloy Theoretic Automated Toolkit (ATAT). Included in ATAT, the MIT Ab-initio Phase Stability (maps) code was used to generate the energy landscapes and CEs. The Easy Monte Carlo Code (emc2 and phb) was used to perform MC simulations to obtain the phase diagrams. With well-converged CEs, a box of 12 × 12 × 12 2-atom unit cells (1728 exchangeable sites) was chosen in the semi-grand canonical (SGC) ensemble simulations, in which chemical potential and temperature (T) can be given as external conditions. Chemical potential is defined as $\mu_i = \left({}^{\partial G}/_{\partial n_i}\right)_{T,n_{j\neq i}}$, where G is the Gibbs free energy, n_i is the number of atoms of species i in the simulation cell. In a binary system $A_{1-x}B_x$, $\mu = \mu_A - \mu_B$ is used as the input. For each μ and T point, sufficient MC passes were used to make sure the composition (x) reached a precision of 0.01. In a SGC ensemble the composition jumps from one boundary to another, skipping the two-phase region in response to the change in μ. This jumping prevents the determination of spinodal curves in this ensemble.

Published work: Z.T.Y. Liu, B.P. Burton, S. V Khare, and D. Gall, *J. Phys. Condens. Matter* **29**, 35401 (2017).

Vickers Hardness

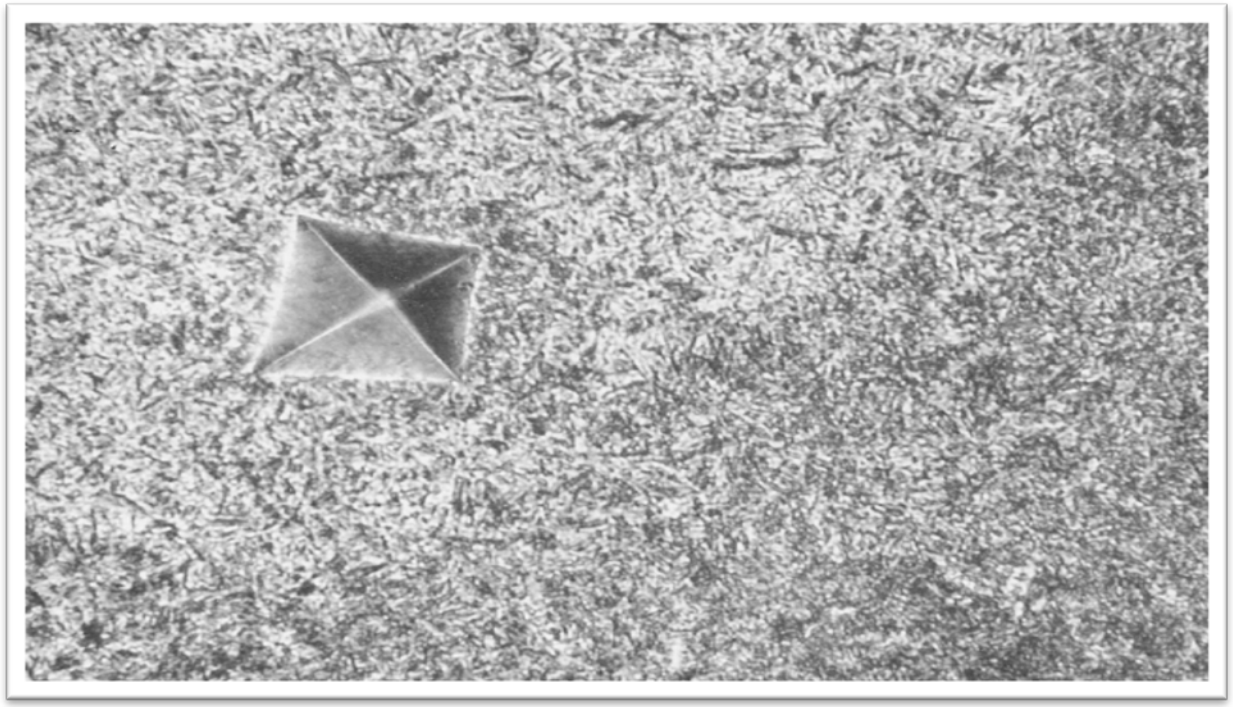

http://en.wikipedia.org/wiki/Vickers_hardness_test

Brittleness/Ductility

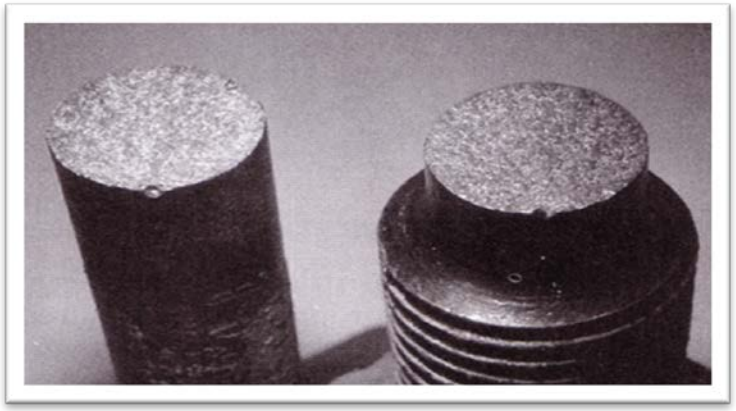

brittle

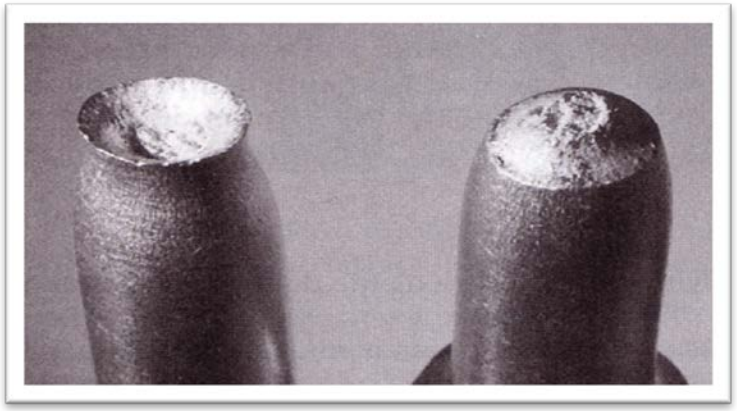

ductile

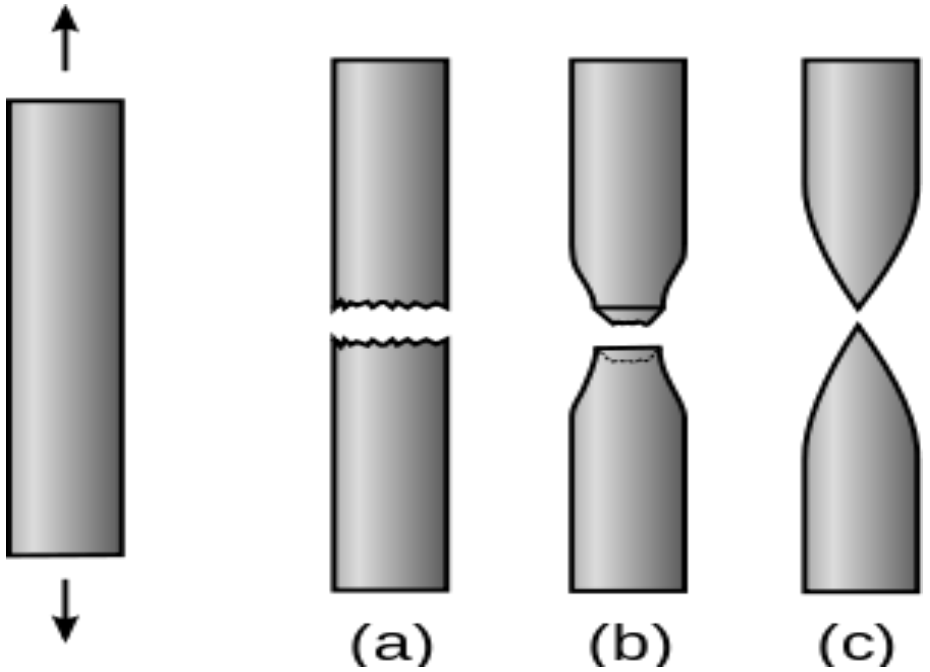

brittle ductile very ductile

http://oregonstate.edu/instruct/engr322/Homework/AllHomework/S09/ENGR322HW7.html
http://en.wikibooks.org/wiki/Advanced_Structural_Analysis/Part_I_-_Theory/General_Properties_of_Materials

Elastic Constants

- There are two ways to determine the elastic constants.
  - Energy-strain
  - Stress-strain
- Here we employed the energy-strain method, which requires fitting the relation to a 2nd order polynomial. The strain tensor has the general form below.
- There are three independent elastic constants, C_{11}, C_{12} and C_{44} for the cubic crystallographic system. Therefore, we applied three sets of strains to the unit cell.

$$\varepsilon_{ij} = \begin{pmatrix} e_1 & \frac{e_6}{2} & \frac{e_5}{2} \\ \frac{e_6}{2} & e_2 & \frac{e_4}{2} \\ \frac{e_5}{2} & \frac{e_4}{2} & e_3 \end{pmatrix}$$

Strain	Non-zero Strain Elements	$\Delta E/V_0$
1	$e_1=e_2=e_3=\delta$	$3/2\ (C_{11}+2C_{12})\delta^2$
2	$e_1=\delta$, $e_2=-\delta$, $e_3=\delta^2/(1-\delta^2)$	$(C_{11}-C_{12})\delta^2$
3	$e_6=\delta$, $e_3=\delta^2/(4-\delta^2)$	$1/2\ C_{44}\delta^2$

Equation for Calculating Vickers Hardness (H_V)

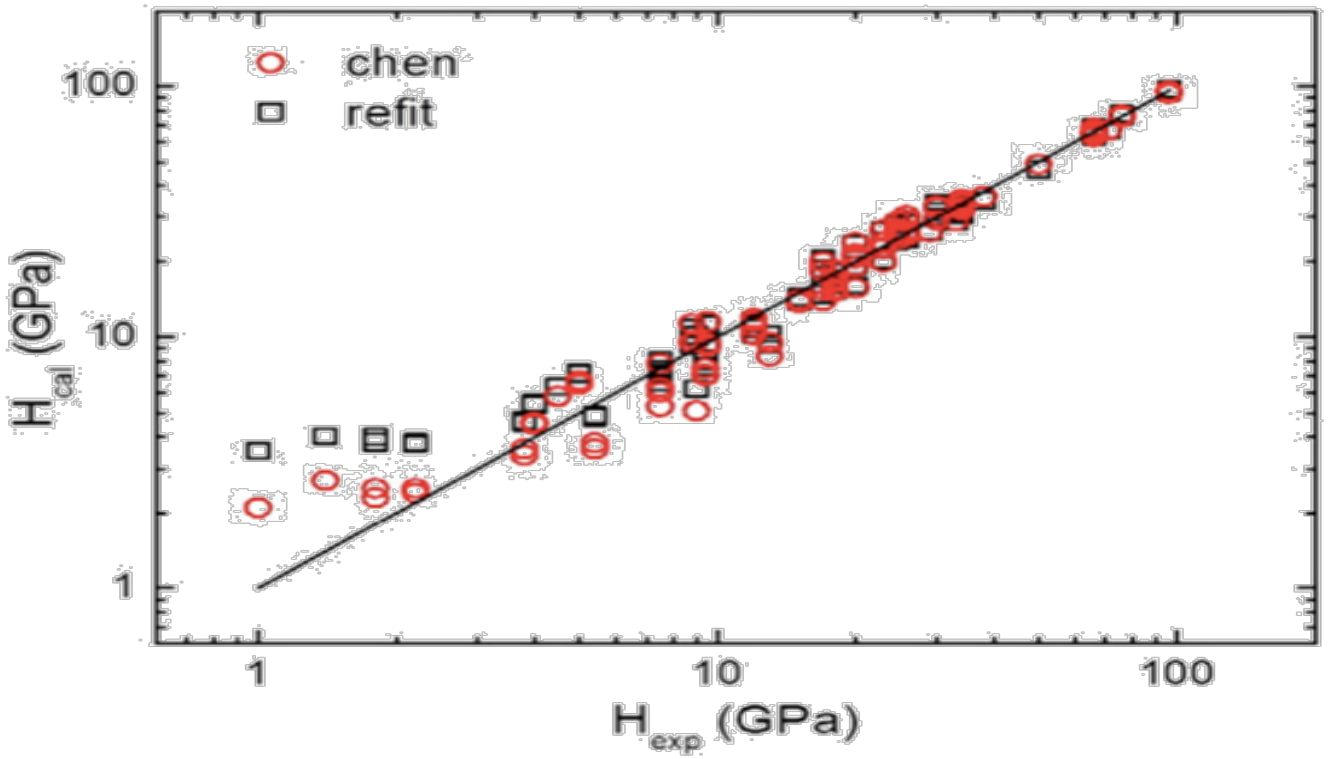

$$H_V = 0.92k^{1.137}G^{0.708}$$

$k = G/B$

k - Pugh's ratio
G - shear modulus

Data points (40+ compounds):

Covalent: C, Si, BN…
Ionic: NaCl, KBr…
Metallic glasses

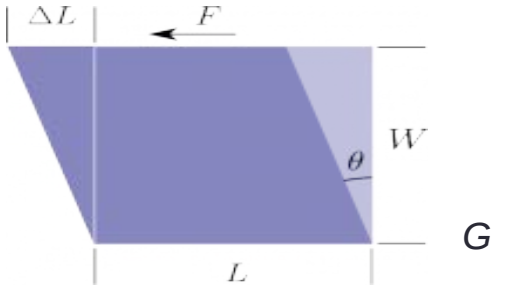

Figure adapted from Tian et al.
Y. Tian, B. Xu, and Z. Zhao, Int. J. Refract. Met. Hard Mater. 33, 93 (2012).
X. Q. Chen, H. Y. Niu, D. Z. Li and Y. Y. Li, *Intermetallics* 19, 1275 (2011).

Anti-Correlation

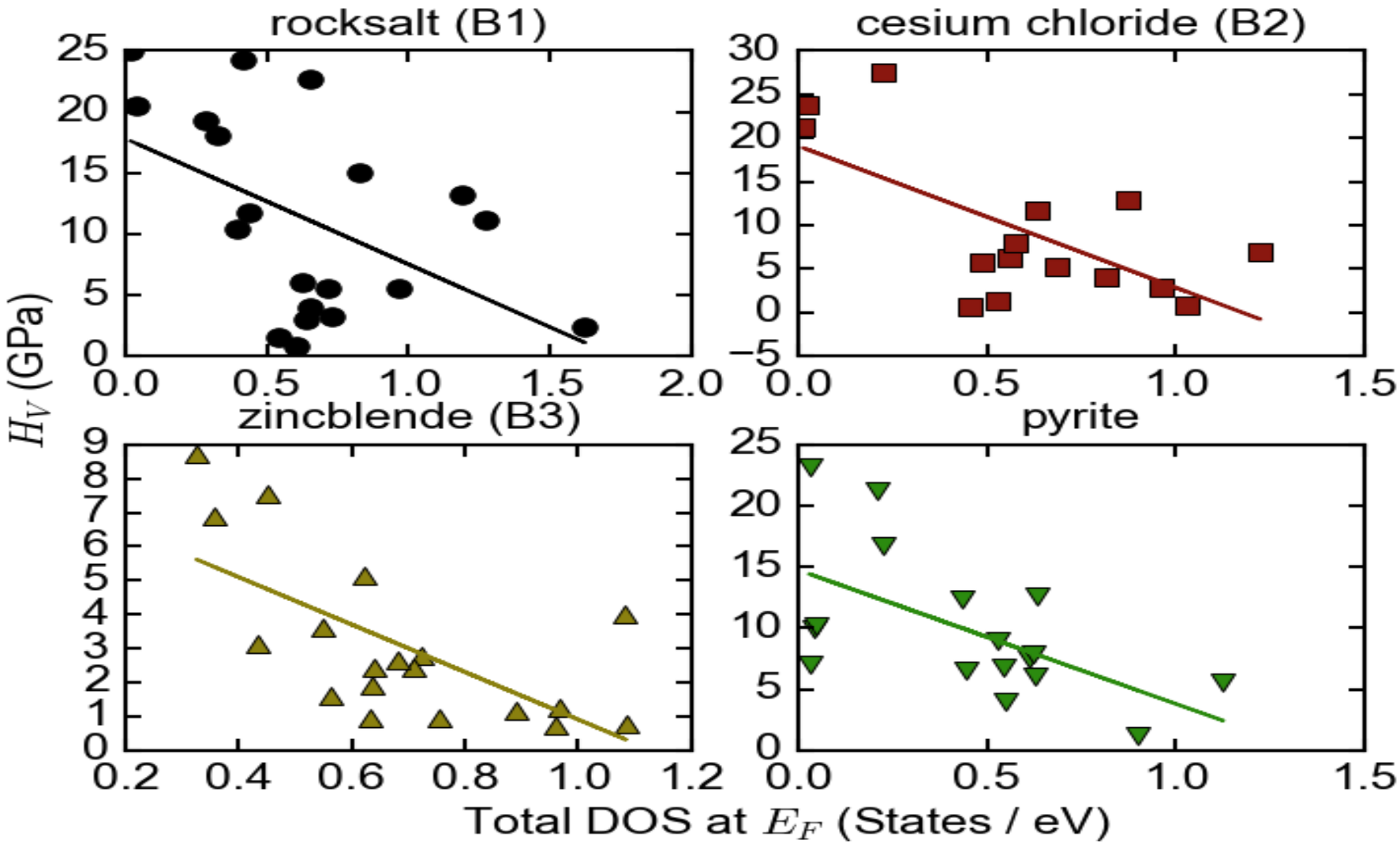

Difference in B and G

$$B = (C_{11} + 2C_{12})/3$$

$$G_V = [(C_{11} - C_{12}) + 3C_{44}]/5$$

$$G_R = [5(C_{11} - C_{12})C_{44}]/[4C_{44} + 3(C_{11} - C_{12})]$$

$$G = G_{VRH} = (G_V + G_R)/2$$

$$k = G/B$$

Difference in *B* and *G*

Bulk modulus (*B*) only measures the resistance to isotropic hydrostatic pressure, while shear modulus (*G*) measures the resistance to anisotropic shear strain.

TiN (*G*: 187.2 GPa, *B*: 318.3 GPa, H_V: 23 GPa)

β-SiC (*G*: 191.4 GPa, *B*: 224.7 GPa, H_V: 34 GPa)

Gao FM, He JL, Wu ED, Lu SM, Yu LD, Li DC, et al. Phys Rev Lett 2003;91: 015502.
Gou HY, Hou L, Zhang JW, Gao FM. Appl Phys Lett 2008;92:241901.

Formulation for H_V (Vickers Hardness)

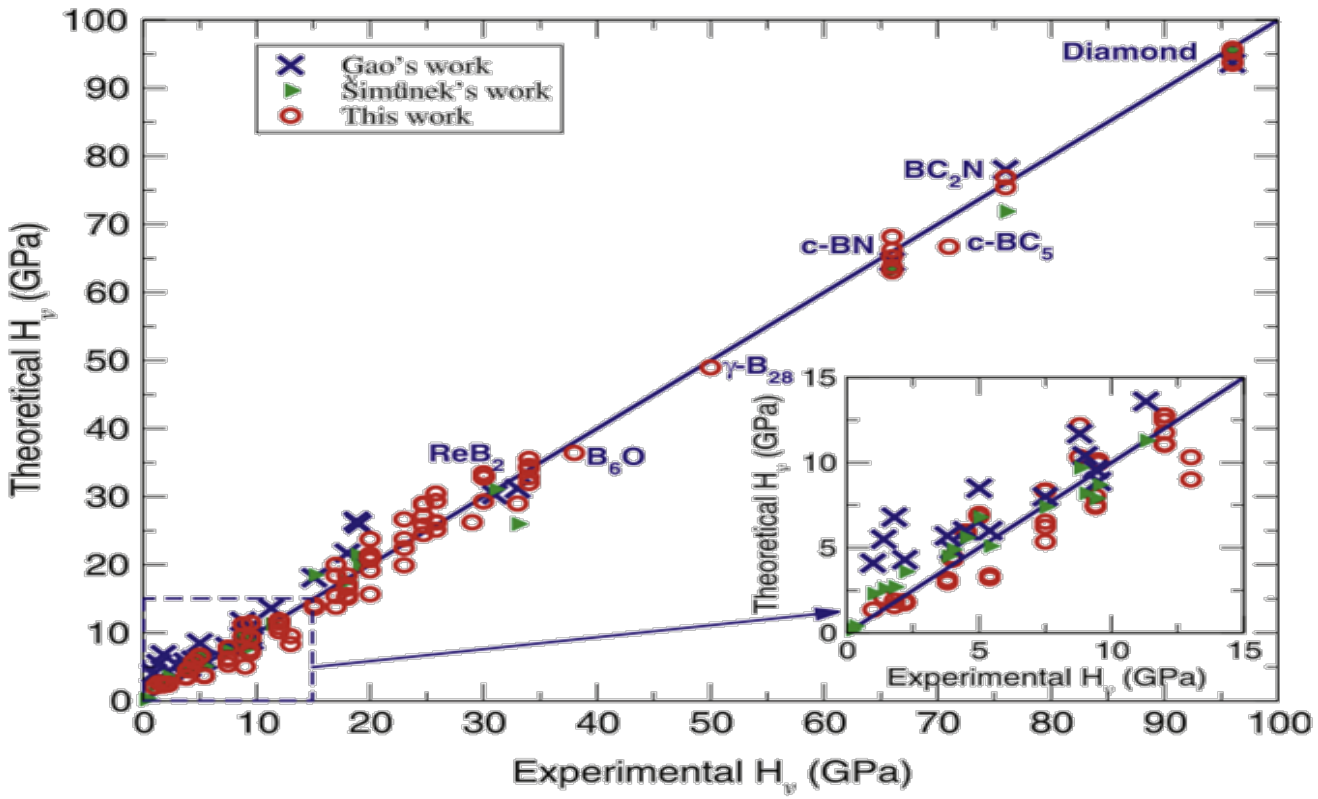

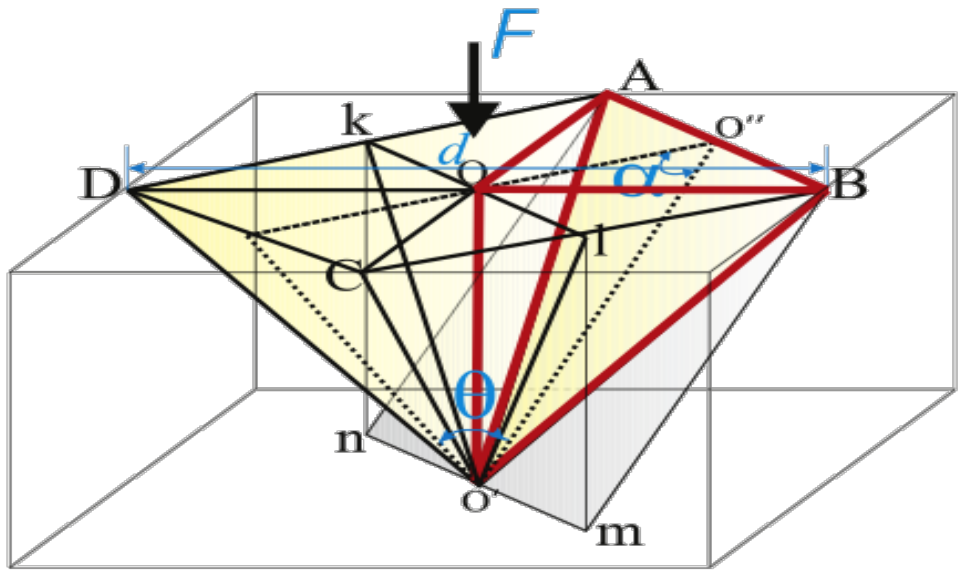

$$H_v = 2\left(k^2 G\right)^{0.585} - 3$$

X. Q. Chen *et al.*, Intermetallics **19**, 1275 (2011)

Crystal	H_{Exp} (GPa)	H_{Tian} (GPa)	$H_{Simunek}$ (GPa)	H_{Xue} (GPa)	H_{Chen} (GPa)
C	96[a]	93.6	95.4[b]	90[e]	94.6[f]
Si	12[a]	13.6	11.3[b]	14[e]	11.2[f]
Ge	8.8[b]	11.7	9.7[b]	11.4[e]	10.4[f]
SiC	31[b]	30.3	31.1[b]	27.8[e]	33.8[f]
BN	63[a]	64.5	63.2[b]	47.7[e]	65.3[f]
BP	33[a]	31.2	26[b]	24.9[e]	29.3[f]
BAs	19[b]	26	19.9[b]	21.1[e]	–
AlN	18[a]	21.7	17.6[b]	14.5[e]	16.8[f]
AlP	9.4[a]	9.6	7.9[b]	7.4[e]	7.2[f]
AlAs	5.0[a]	8.5	6.8[b]	6.3[e]	6.6[f]
AlSb	4.0[a]	4	4.9[b]	4.9[e]	4.4[f]
GaN	15.1[a]	18.1	18.5[b]	13.5[e]	13.9[f]
GaP	9.5[a]	8.9	8.7[b]	8[e]	9.9[f]
GaAs	7.5[a]	8	7.4[b]	7.1[e]	7.8[f]
GaSb	4.5[a]	6	5.6[b]	4.5[e]	5.8[f]
InN	9[a]	10.4	8.2[b]	7.4[e]	7.4[f]
InP	5.4[a]	6	5.1[b]	3.9[e]	3.7[f]
InAs	3.8[a]	3.8	5.7[b]	4.5[e]	3.3[f]
InSb	2.2[a]	4.3	3.6[b]	2.2[e]	2.4[f]
ZnS	1.8[b]	6.8	2.7[b]	2.4[e]	2.4[f]
ZnSe	1.4[b]	5.5	2.6[b]	1.8[e]	2.7[f]
ZnTe	1[b]	4.1	2.3[b]	0.9[e]	2.1[f]
TiC	32[c]	34	18.8[b]	23.9[e]	27[f]
TiN	20.6[c]	21.6	18.7[b]	23.8[h]	23.3[f]
ZrC	25[c]	21	10.7[g]	15.7[h]	27.5[f]

Y. Tian *et al.*, Int. J. Refract. Met. Hard Mater. **33**, 93 (2012).

Crystal	H_{Exp} (GPa)	H_{Tian} (GPa)	$H_{Simunek}$ (GPa)	H_{Xue} (GPa)	H_{Chen} (GPa)
ZrN	15.8[c]	16.7	10.8[g]	15.9[h]	–
HfC	26.1[c]	26.8	10.9[g]	15.6[h]	–
HfN	16.3[c]	18	10.6[g]	15.2[h]	19.2[f]
VC	27.2[c]	23	25.2[g]	17.5[h]	26.2[f]
VN	15.2[c]	14.9	26.5[g]	16.5[h]	–
NbC	17.6[c]	16.1	18.3[b]	12.8[h]	15.4[f]
NbN	13.7[c]	13.6	19.5[b]	12[h]	14.7[f]
TaC	24.5[c]	26	19.9[g]	14.7[h]	–
TaN	22[c]	20	21.2[g]	14.3[h]	–
CrN	11[c]	11	36.6[g]	19.2[h]	–
WC	30[c]	31	21.5[b]	20.6[e]	31.3[f]
Re_2C	17.5[j]	19.7[j]	11.5[g]	16.2[h]	26.4[i]
Al_2O_3	20[c]	18.8	13.5[g]	18.4[h]	20.3[i]
MgO	3.9[d]	4.5	4.4[g]	5.4[h]	24.8[i]
LiF	1[d]	0.8	2.2[g]	–	8.5[i]
NaF	0.6[d]	0.85	1[g]	–	5.7[i]
NaCl	0.2[d]	0.4	0.4[b]	–	2.4[i]
KCl	0.13[d]	0.18	0.2[b]	–	2.3[i]
KBr	0.1[d]	0.23	0.2[g]	–	0.1[i]

[a] Reference [34].
[b] Reference [37].
[c] Reference [32].
[d] Reference [60].
[e] Reference [58].
[f] Reference [30].
[g] Calculated by authors using method [36].
[h] Caculated using [35].
[i] Calculated with [30].
[j] Referenece [52].

k vs P_C

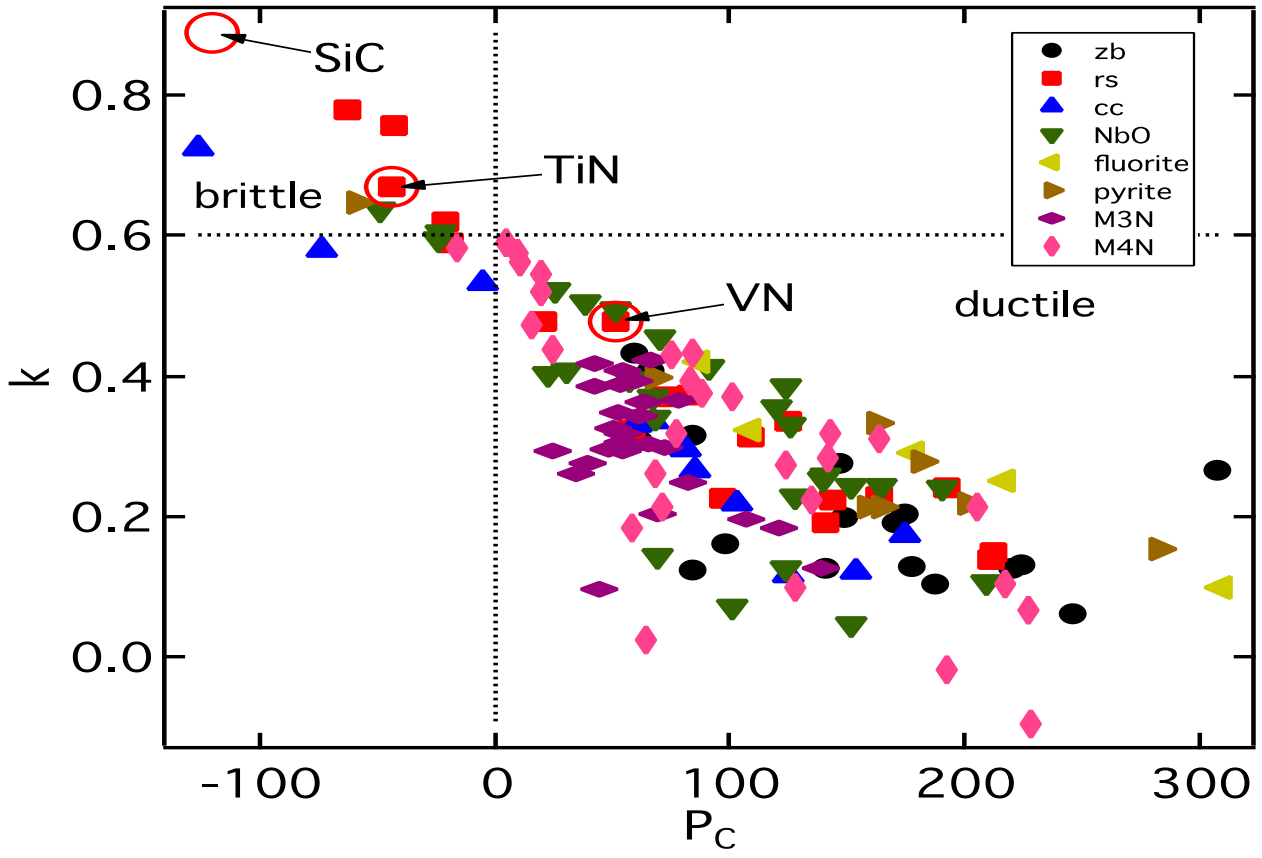
SiC
TiN
VN
brittle
ductile
zb
rs
cc
NbO
fluorite
pyrite
M3N
M4N
k
0.8
0.6
0.4
0.2
0.0
-100
0
100
200
300
P_C

Chen's formulation for calculating H_V (Vicker's Hardness)

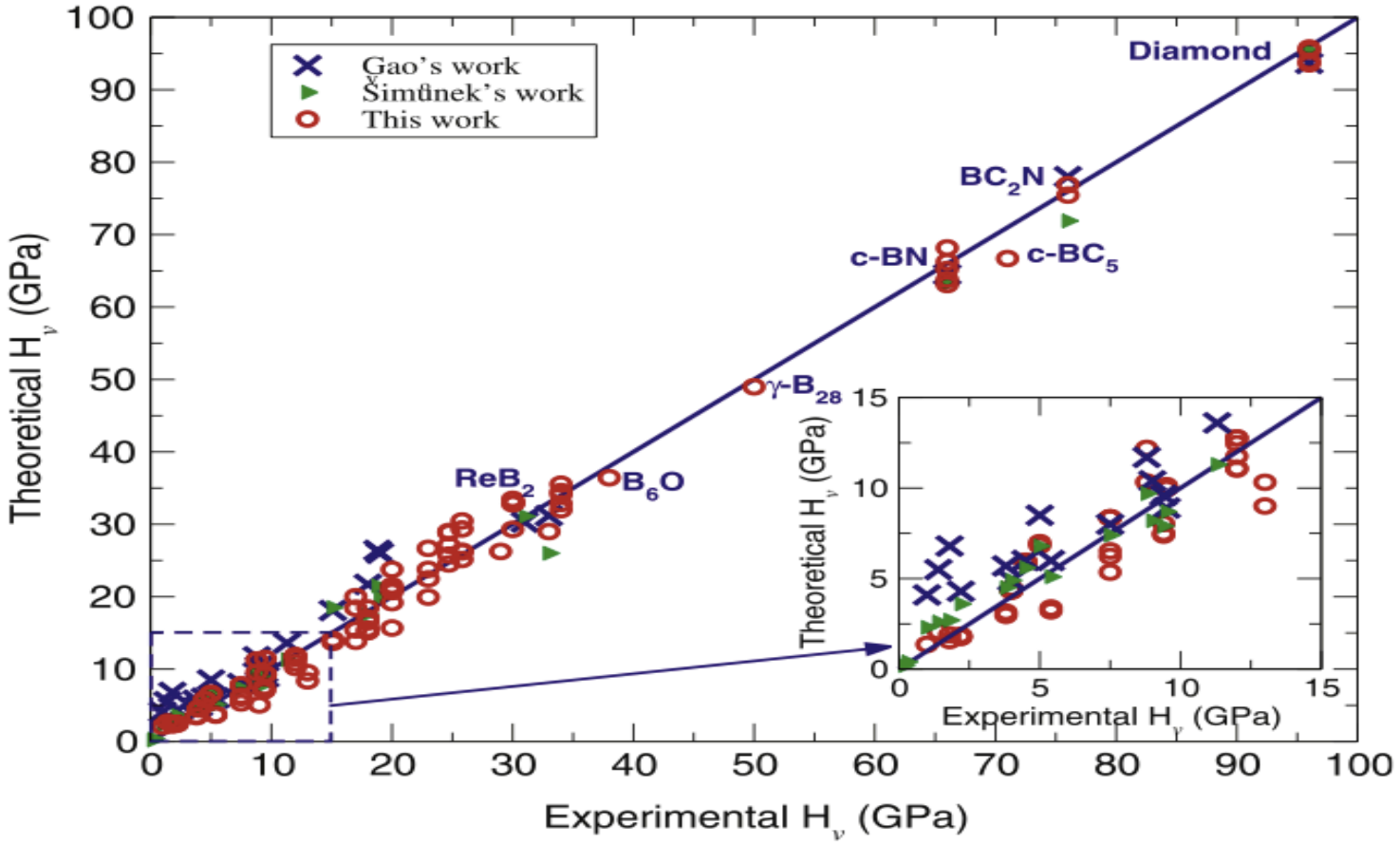

$B = (C_{11} + 2C_{12})/3$

$G_v = [(C_{11} - C_{12}) + 3C_{44}]/5$

$G_R = [5(C_{11} - C_{12})C_{44}]/(4C_{44} + 3C_{11} - 3C_{12})$

$G = G_{VRH} = (G_v + G_R)/2$

$k = G/B$

$$H_v = 2\left(k^2 G\right)^{0.585} - 3$$

X. Q. Chen *et al.*, Intermetallics **19**, 1275 (2011)

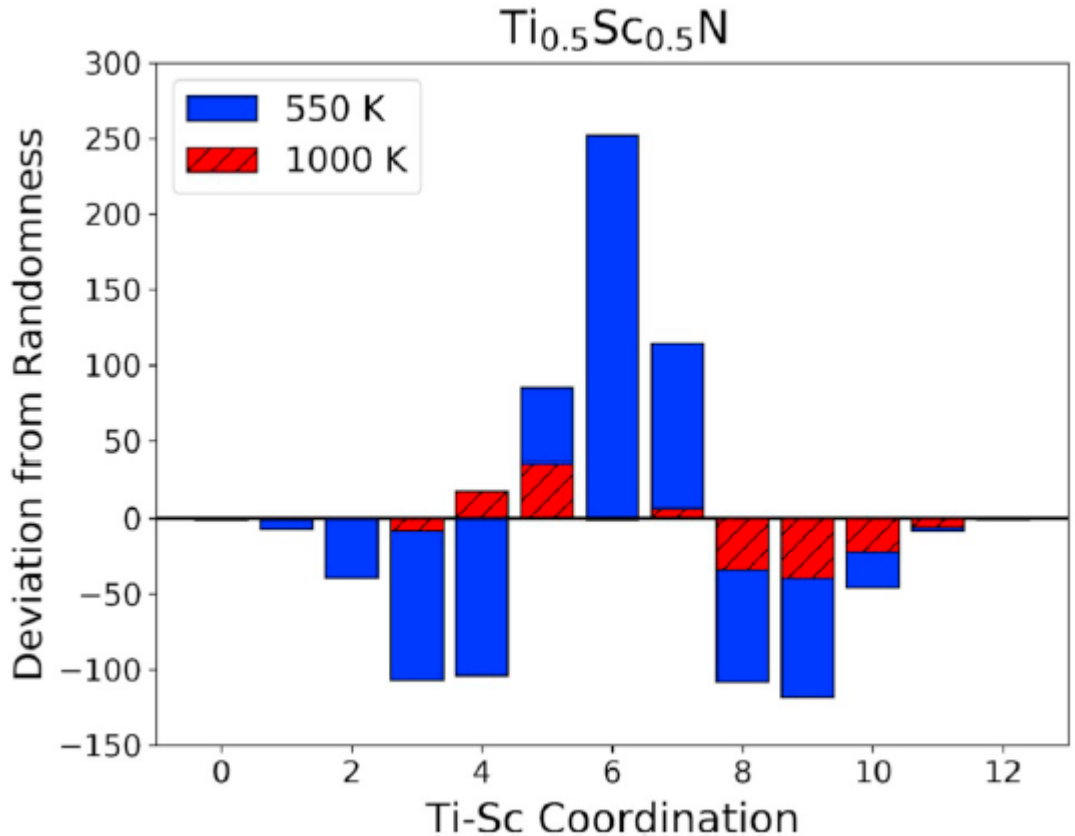
$Ti_{0.5}Sc_{0.5}N$
550 K
1000 K
Deviation from Randomness
300
250
200
150
100
50
0
−50
−100
−150
0
2
4
6
8
10
12
Ti-Sc Coordination

Crystal Field Splitting

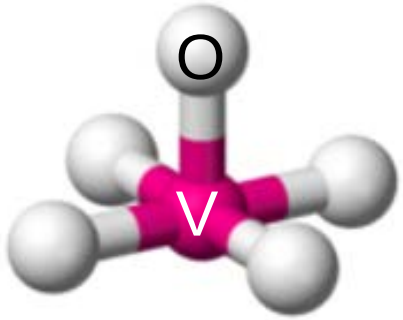

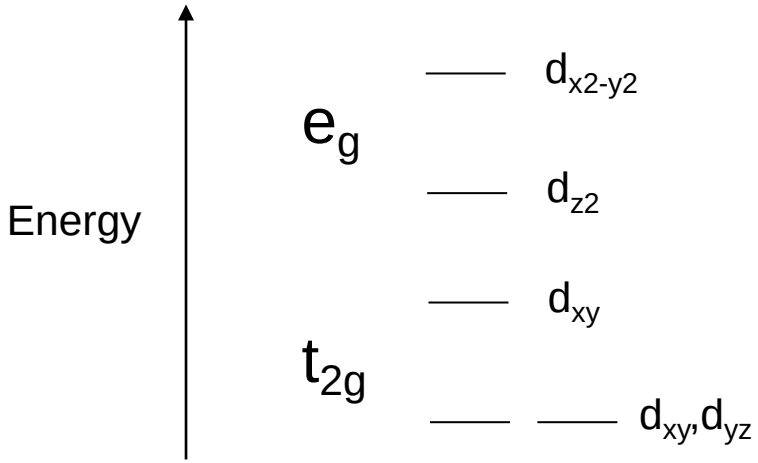

- Square-pyramidal
- e_g above t_{2g}

- Tetrahedral
- t_{2g} above e_g